Journal of Visualized Experiments

Combined use of tail vein metastasis assays and real-time in vivo imaging to quantify breast cancer metastatic colonization and burden in the lungs

--Manuscript Draft--

1 **TITLE:**
2 Combined Use of Tail Vein Metastasis Assays and Real-Time In Vivo Imaging to Quantify Breast
3 Cancer Metastatic Colonization and Burden in the Lungs
4
5 **AUTHORS AND AFFILIATIONS:**
6 Janine S. A. Warren[1], Paul J. Feustel[2], John M. Lamar[1]
7
8 [1] Department of Molecular and Cellular Physiology, Albany Medical College, Albany, NY, USA
9 [2] Department of Neuroscience and Experimental Therapeutics, Albany Medical College, Albany,
10 NY, USA
11
12 **Email addresses of co-authors:**
13 Janine S. A. Warren   (warrenj1@amc.edu)
14 Paul J. Feustel   (feustep@amc.edu)
15
16 **Corresponding author:**
17 John M. Lamar   (lamarj@amc.edu)
18

19 **KEYWORDS:**
20 4T1 cells, syngeneic mouse model, metastasis, metastatic colonization, breast cancer, mouse,
21 live animal imaging, tail vein metastasis, YAP, TAZ.
22

23 **SUMMARY:**
24 The described approach combines experimental tail vein metastasis assays with in vivo live
25 animal imaging to allow real-time monitoring of breast cancer metastasis formation and growth
26 in addition to the quantification of metastasis number and size in the lungs.
27
28 **ABSTRACT:**
29 Metastasis is the main cause of cancer-related deaths and there are limited therapeutic options
30 for patients with metastatic disease. The identification and testing of novel therapeutic targets
31 that will facilitate the development of better treatments for metastatic disease requires
32 preclinical in vivo models. Demonstrated here is a syngeneic mouse model for assaying breast
33 cancer metastatic colonization and subsequent growth. Metastatic cancer cells are stably
34 transduced with viral vectors encoding firefly luciferase and ZsGreen proteins. Candidate genes
35 are then stably manipulated in luciferase/ZsGreen-expressing cancer cells and then the cells are
36 injected into mice via the lateral tail vein to assay metastatic colonization and growth. An in vivo
37 imaging device is then used to measure the bioluminescence or fluorescence of the tumor cells
38 in the living animals to quantify changes in metastatic burden over time. The expression of the
39 fluorescent protein allows the number and size of metastases in the lungs to be quantified at the
40 end of the experiment without the need for sectioning or histological staining. This approach
41 offers a relatively quick and easy way to test the role of candidate genes in metastatic
42 colonization and growth, and provides a great deal more information than traditional tail vein
43 metastasis assays. Using this approach, we show that simultaneous knockdown of Yes associated
44 protein (YAP) and transcriptional co-activator with a PDZ-binding motif (TAZ) in breast cancer

45   cells leads to reduced metastatic burden in the lungs and that this reduced burden is the result
46   of significantly impaired metastatic colonization and reduced growth of metastases.
47
48   **INTRODUCTION:**
49   Cancer remains the second leading cause of death worldwide[1] and metastasis is responsible for
50   the majority of these deaths[2,3]. However, a limited understanding of the molecular mechanisms
51   that govern metastatic colonization and subsequent growth has hindered the development of
52   effective treatments for metastatic disease. The identification of novel therapeutic targets
53   requires an assay to test how perturbed expression or function of a candidate gene influences
54   metastasis formation and growth. While autochthonous mouse models have their advantages,
55   they are time-consuming and expensive to generate, making them more suited for target
56   validation rather than target discovery. Transplant model systems in which the candidate gene is
57   perturbed in cancer cells in vitro and then effects on metastatic potential are assessed in vivo,
58   are less expensive and higher throughput than autochthonous models. In addition, viral vectors
59   for stable delivery of RNAi, CRISPR/CAS9, and transgenes are widely available, making it relatively
60   easy to perturb virtually any gene or genes of interest in a cancer cell lines. This approach can
61   also be used to assay the role of candidate genes in metastatic colonization and growth in human
62   cancer cell lines by transplanting the cells into immunocompromised or humanized mice.
63
64   The two types of assays used to test metastasis formation by transplanted cancer cells in vivo are
65   spontaneous metastasis assays and experimental metastasis assays. In spontaneous metastasis
66   assays[4,5], cancer cells are injected into mice, allowed to form a primary tumor, and then
67   spontaneous metastasis formation and subsequent growth are assayed. The strength of this
68   model is that the cells must complete all steps of the metastatic process in order to form
69   metastatic tumors. However, many cancer cell lines do not metastasize efficiently in spontaneous
70   metastasis models, and any manipulation of the cells that impacts primary tumor growth can
71   confound the results of the metastasis assay. Experimental metastasis assays, in which cancer
72   cells are injected directly into circulation, are used to avoid these pitfalls. Common experimental
73   metastasis assays include the tail vein injection[6-8] (and demonstrated here), intracardiac
74   injection[9], and portal vein injection[10].
75
76   The purpose of the protocol presented here is to provide an in vivo experimental metastasis assay
77   that allows a researcher to monitor metastasis formation and growth in real time, as well as to
78   quantify end point metastasis number and size in the lungs of the same mouse. To accomplish
79   this, traditional experimental tail vein metastasis assays[6-8] are combined with live animal imaging,
80   using an in vivo imaging device[9,11-14]. Tumor cells stably expressing both luciferase and a
81   fluorescent protein are injected into mice via the lateral tail vein and then the in vivo imaging
82   device is used to measure changes in metastatic burden in the lungs over time (**Figure 1**).
83   However, the in vivo live animal imaging device cannot distinguish or measure the size of
84   individual metastases. Thus, at the end of the experiment, a fluorescent stereomicroscope is used
85   to count the number and measure the size of the fluorescent metastases in the lungs without the
86   need for sectioning and histology or immunohistochemistry (**Figure 1**). This protocol can be used
87   to test how altering the expression or function of a candidate gene influences metastasis
88   formation and growth. Potential therapeutic compounds such as small molecules or function

89   blocking antibodies can also be tested.
90
91   To demonstrate this approach, we first performed a proof of concept experiment in which the
92   essential replication factor, replication protein A3 (RPA3) is knocked down in metastatic mouse
93   breast cancer cells. We show that mice injected with RPA3 knockdown cells have significantly less
94   metastatic burden at every time point compared to mice injected with control cells. Analysis of
95   the metastasis-containing lungs shows that this reduced metastatic burden is the result of
96   significantly reduced metastatic colonization and impaired growth of the metastases that form.
97   To further demonstrate this technique, we tested whether simultaneous knock down of Yes
98   associated protein (YAP) and transcriptional co-activator with a PDZ-binding motif (TAZ) impairs
99   metastatic colonization or subsequent growth. YAP and TAZ are two related transcriptional co-
100   activators that are the critical downstream effectors of the Hippo Pathway. We[15,16] and others
101   have implicated YAP and TAZ in metastasis (reviewed in[17-19]), suggesting that these proteins are
102   good therapeutic targets. Consistently, we found that mice injected with YAP/TAZ knockdown
103   cells had significantly reduced metastatic burden. Analysis of the lungs showed that the YAP/TAZ
104   knockdown cells formed many fewer metastases and that the metastases that did form were
105   smaller. These experiments demonstrate how experimental metastasis assays allow a researcher
106   to quickly and inexpensively test the role of a candidate gene in metastasis formation and growth.
107   They further show how the combined use of live animal imaging and fluorescent quantification
108   of metastases in whole lungs allows the researcher to better understand the steps during
109   metastatic colonization.
110
111   **PROTOCOL:**
112   This protocol involves the use of mice and biohazardous materials and requires approval from
113   the appropriate institutional safety committees. All of the described in vivo work here is
114   approved by the Albany Medical College institutional animal care and use committee (IACUC).
115
116   NOTE: For a protocol overview, see schematic in **Figure 1**.
117
118   1. **Packaging all required retroviruses and lentiviruses**
119
120   NOTE: The described protocol uses lentiviral or retroviral vectors to stably express a luciferase
121   enzyme and fluorescent protein as well as to manipulate the expression of a candidate gene.
122   These viruses are packaged in HEK-293FT cells as described below.
123
124   1.1. Day 1: Plate HEK-293FT cells on 6-well plates in 2 mL of complete growth media (10% FBS in
125   DMEM with 1% penicillin/streptomycin and 2 mM L-Glutamine) so that they are 40-60%
126   confluent on day 2. Incubate at 37 °C, 5% CO_2 overnight.
127
128   1.2. Day 2: For each viral vector to be packaged, transfect a 40-60% confluent well of HEK-293FT
129   cells with the retroviral or lentiviral vector and the appropriate vectors encoding the viral coat
130   and packaging proteins.
131
132   NOTE: This protocol uses VSVG as the coat protein, psPAX2 for lentiviral packaging, and gag-pol

133   for retroviral packaging (see **Supplemental Table 1** for vector list).
134
135   1.3. Make a co-transfection mixture for each well as follows:
136
137   1.3.1. Combine 4 µL of lipid solution for transfections (see **Table of Materials**) and 96 µL of
138   transfection buffer and incubate for 5 minutes.
139
140   1.3.2. Add 1 µg of viral vector, 0.5 µg of coat protein vector (VSVG), and 0.5 µg of packaging
141   protein vector (psPAX2 or gag-pol) and incubate for 20 minutes.
142
143   1.3.3. Gently add the co-transfection mixture from step 1.3.2 to the HEK-293FT cells plated in
144   step 1.1 and incubate at 37 °C, 5% CO_2 overnight.
145
146   1.4. Day 3: Remove the transfection-containing media from each well and gently add 2 mL of
147   complete growth media to each well. Incubate at 37 °C, 5% CO_2 for approximately 24 hours.
148
149   1.5. Day 4: Collect the viral supernatant from each well using a 3 mL syringe and filter through a
150   0.45 µm filter into a 2 mL microcentrifuge tube.
151
152   1.6. Optional: If collection of a second batch of virus is desired, gently add 2 mL of complete
153   growth media to each well and incubate at 37 °C, 5% CO_2 for approximately 24 hours.
154
155   1.7. Day 5 (Optional): Collect a second round of viral supernatant as in step 1.5.
156
157   NOTE: The protocol may be paused by freezing the viral supernatant.
158
159   2. **Generation of cancer cells stably expressing luciferase and a fluorescent protein**
160
161   NOTE: The following protocol describes how to first to stably label 4T1 cells with firefly luciferase
162   and a fluorescent protein (ZsGreen) using two vectors with unique selection genes. Then a 3rd
163   viral vector is used to manipulate the expression of a candidate gene. However, viral vectors that
164   simultaneously deliver a fluorescent protein and a genetic manipulation can also be used as an
165   alternative (as in the representative experiments below). Other cancer cells can be used, but the
166   cell numbers should be optimized for steps 2.1 and 2.7.1.
167
168   2.1. Plate 4T1 cells at 1.5 x 10^5 cells/well in a 12-well plate in complete growth media (10% FBS
169   in DMEM with 1% penicillin/streptomycin and 2 mM L-Glutamine) and incubate at 37 °C, 5% CO_2
170   overnight.
171
172   2.2. Infect the 4T1 cells with the viral supernatant generated in step 1 as follows.
173
174   2.2.1. Aspirate the growth media from the cells and add 500 µL of luciferase viral supernatant
175   and 500 µL of fluorescent protein viral supernatant to simultaneously infect the cells with both
176   the luciferase and fluorescent protein viral supernatants.

177

178   2.2.2. Add 1 µL of 8 mg/mL hexadimethrine bromide (see **Table of Materials**).

179

180   2.2.3. Incubate the cells at 37 °C, 5% until 75-90% confluent (typically 24-48 hours).

181

182   2.3. Trypsinize the 4T1 cells with 500 µL of trypsin for 2-5 minutes (cells should freely rinse off
183   the bottom of the well). Transfer all the cells to a 6 cm dish in 4 mL of selection media (complete
184   growth media containing the appropriate antibiotics) thereby quenching the trypsin. Plate a 6 cm
185   dish of non-infected control cells in the same selection media.

186

187   NOTE: Appropriate antibiotic concentration should be determined ahead of time by testing
188   several doses. Additionally, fluorescence-activated cell sorting can also be used to select the
189   fluorescently labeled cells in place of drug selection.

190

191   2.4. Incubate the cells at 37 °C, 5% CO_2 in selection media and split the cells when necessary until
192   all non-infected control cells are dead (dependent upon the selection gene and cell line).

193

194   2.5. Confirm that the infected 4T1 cells are expressing the ZsGreen fluorescent protein using an
195   MB-1 filter block (excitation D540/25x) filter on an inverted fluorescent microscope at 100x
196   magnification.

197

198   2.6. Confirm that the infected 4T1 cells are expressing luciferase using a commercially available
199   luciferase activity kit as follows.

200

201   2.6.1. Use a minimal volume of 1x passive lysis buffer to lyse luciferase-expressing 4T1 cells and
202   control 4T1 cells that do not express luciferase, gently shaking for 30 minutes.

203

204   2.6.2. Add 20 µL of cell lysate to a white-bottom 96-well plate and then 50 µL of the luciferase
205   assay reagent from the luciferase activity kit.

206

207   2.6.3. Use a plate reader to measure the luminescence from the cells at all wavelengths in the
208   spectrum by using the luminescence setting.

209

210   NOTE: The protocol may be paused by freezing down the stably-transduced cells.

211

212   2.7. Manipulate the expression of the candidate gene as follows:

213

214   2.7.1. Plate 6 x 10^5 labeled 4T1 cells from step 2.6 on a 60 mm dish in 4 mL of complete growth
215   media and incubate at 37 °C, 5% CO_2 overnight.

216

217   2.7.2. Aspirate the growth media from each well and add 2 mL of complete growth media
218   containing 4 µL of 8 mg/mL hexadimethrine bromide.

219

220   2.7.3. Add 2 mL of viral supernatant from step 1 to the cells plated from step 2.7.2 and incubate

221   at 37 °C, 5% CO_2 overnight.

222

223   2.7.4. Trypsinize the 4T1 cells with 500 µL of trypsin for 2-5 minutes (cells should freely rinse off
224   the bottom of the well). Transfer all of the cells to a 10 cm dish in 10 mL of selection media
225   (complete growth media containing the appropriate antibiotics) thereby quenching the trypsin.
226   Plate some non-infected control labeled 4T1 cells in the same selection media.

227

228   2.7.5. Incubate the cells at 37 °C, 5% CO_2 in selection media and split the cells when necessary
229   until all non-infected cells are dead.

230

231   2.7.6. Confirm that the expression of the candidate gene is altered using a standard approach
232   such as western blot[20] or qPCR[21].

233

234   2.7.7. Assay luminescence and fluorescence as in steps 2.5-2.6 to determine how similar they are
235   in control and knockdown cells, as this can change (see Discussion).

236

237   NOTE: The protocol may be paused by freezing down the stably-transduced cells.

238

239   3. **Optimization of the in vivo experimental design**

240

241   3.1. Optimize appropriate cell number and duration of experiment for the desired metastatic
242   burden as follows.

243

244   3.1.1. Expand the fluorescent and bioluminescent 4T1 cells from step 2.6 in complete growth
245   media so that excess cells are available on the desired day of injection.

246

247   3.1.2. Prepare the cells for tail vein injections as described in step 4.2. To determine the optimal
248   cell number for injections, resuspend the cells at several different concentrations in 100 µL of 1x
249   PBS.

250

251   NOTE: We recommend testing a range of cell numbers/mouse from 25,000 up to 500,000.

252

253   3.1.3. Keep the cell suspensions on ice until injection.

254

255   3.1.4. Inject each dilution of 4T1 cells from step 3.1.2 into 3-4 mice via the lateral tail vein
256   described in step 4.3 (see below).

257

258   3.1.5. Return the mouse to its cage and monitor for 15 minutes to ensure a full recovery. Mice
259   should be checked for signs of pain or distress 3x weekly.

260

261   3.1.6. Monitor mice for metastasis formation and growth for 3-6 weeks (cell line and mouse
262   strain dependent) using an in vivo live animal imaging device (see steps 5 and 6).

263

264   3.1.6.1. Euthanize mice 3-6 weeks after the tail vein injection according to standard institutional

265 guidelines.

267 3.1.6.2. Prepare the lungs and assess metastasis size and number described in step 7.

269 3.1.6.3. Choose the appropriate length of time for the metastases to grow for the desired
270 metastatic burden (see discussion).

272 4. **Tail vein injection of labeled cancer cells**

274 NOTE: Step 4.2.4 has been optimized for 4T1 cells growing in syngeneic BALB/c mice. If other
275 cancer cell lines and mouse strains are used, the number of cells injected, and the length of the
276 assay should first be optimized.

278 4.1. Expand the 4T1 cell lines generated in step 2 on two 15 cm dishes in complete growth media
279 so that excess cells are available on the day of injection.

281 4.2. Prepare the cells for tail vein injection as follows:

283 4.2.1. Aspirate the media and rinse the cell plates with 1x PBS.

285 4.2.2. Trypsinize the cells with 5 mL of trypsin per 15 cm plate for 2-5 minutes (cells should freely
286 rinse off the bottom of the well). Transfer all of the cells to a conical tube. Wash remaining cells
287 from the tissue culture dish with enough complete growth media to quench the trypsin and add
288 the wash to the same conical tube.

290 4.2.3. Count the cells using an automated cell counter to determine the total cell number.

292 4.2.4. Centrifuge the cells at 122 x g for 3 minutes, aspirate the supernatant, and resuspend the
293 cells in 1x PBS at the desired concentration. Here, 2.5 x 10^4 cells are injected into each mouse in
294 100 µL of PBS, so the resuspend cells at 2.5 x 10^5 cells/mL. Keep the cell suspensions on ice until
295 injection.

297 NOTE: it is important to limit the amount of time between trypsinization of the cells and the tail
298 vein injection to roughly 1 hour.

300 4.3. Inject 4T1 cells from step 4.2.5 into mice via the lateral tail vein as follows:

302 4.3.1. Gently but thoroughly mix the cells by inverting the tube or using a 1 mL syringe to ensure
303 that they are uniformly resuspended. Always ensure the cells are resuspended prior to loading
304 the syringe.

306 4.3.2. Load a 1 mL Luer-lock syringe with cell suspension and expel excess air bubbles. Place a ½
307 inch, 30-gauge needle on the syringe with the bevel up and expel air bubbles.

308

309   4.3.3. Gently place the mouse in a rodent restrainer.

310

311   4.3.4. The lateral tail veins should be visible and dilated. If not, gently pinch the base of the tail
312   and dip the tail in warm tap water to dilate the veins.

313

314   NOTE: Dilation of the veins may also be achieved by placing the mouse cage under a heating lamp
315   and/or on top of a heating pad.

316

317   4.3.5. Use an alcohol wipe to clean the tail. Insert the needle into the tail vein, bevel side up, and
318   inject 100 µL of cell suspension.

319

320   NOTE: If the needle is inserted properly into the vein, it should easily slide slightly forward and
321   back, and there should not be resistance when the plunger is pushed. Successful injections should
322   also result in a "flush" in which the blue color of the vein turns white for a few seconds following
323   the injection.

324

325   4.4. Slowly remove the needle and using a sterile gauze, apply pressure to the injection site to
326   stop any bleeding.

327

328   4.5. Return the mouse to its cage and monitor for 15 minutes to ensure full recovery. Mice should
329   be checked for signs of pain or distress 3x weekly.

330

331   4.6. Monitor mice for metastasis formation and growth for 3-6 weeks (cell line and mouse
332   strain dependent) using an in vivo live animal imaging device (see steps 5 and 6).

333

334   5. **Monitoring the metastatic burden by fluorescence with an in vivo live animal imaging device**

335

336   NOTE: Do not image animal for fluorescence with active luminescent signal.

337

338   5.1. If only imaging bioluminescence, skip to step 6.

339

340   5.2. Turn on the in vivo live animal imaging device.

341

342   5.3. Set up the in vivo live animal imaging anesthesia system according to manufacturer's
343   guidelines to deliver between 1.5% and 2% isoflurane to the anesthesia chamber and the imaging
344   chamber.

345

346   5.4. Anesthetize mice with fluorescently labeled metastases from step 4 by placing them in an
347   anesthesia chamber and delivering 1.5-2.5% isoflurane.

348

349   5.5. Open the image software (see **Table of Materials**) and login.

350

351   5.6. Click the **Initialize** button and wait for the machine to initialize and for the software to
352   indicate that the camera has reached the appropriate temperature.

5.7. Change the **Field of View** to **D**.

NOTE: **Field of View** C can also be used if a closer view of a mouse is required, but this limits the number of mice that can be imaged simultaneously.

5.8. Click the **Imaging Wizard** button, choose **Fluorescence** and then choose the appropriate filter pair from the drop-down menu.

NOTE: If the fluorophore being used is not an option, choose **Input EX/EM** and type the excitation and emission required.

5.9. Place the mouse in the chamber as described in step 3.2.4.

5.10. Click **Acquire Sequence**.

5.11. After imaging, return the mouse to its cage and monitor for 15 minutes to ensure full recovery.

5.12. Repeat step 5.2 and steps 5.7-5.9 with at least one mouse that does not contain metastases. NOTE: This mouse will be used to quantify and subtract background signal during analysis (step 8).

5.13. Image 2-3 times weekly for the duration of the experiment.

6. **Monitoring the metastatic burden by bioluminescence with an in vivo live animal imaging device**

6.1. Turn on the in vivo live animal imaging device and setup the program as follows.

6.1.1. Open the image software (see **Table of Materials**) and login. Click the **Initialize** button and wait for the machine to initialize and for the software to indicate that the camera has reached the appropriate temperature. Change the **Field of View** to **D**.

NOTE: **Field of View** C can be used for a closer view to image the full mouse body; however, this limits the number of mice that can be imaged at once.

6.1.2. For first time use, edit exposure settings as follows: click **Edit | Preferences | Acquisition | Auto Exposure** and change the maximum exposure time from the default 60 seconds to 300 seconds and click **OK**.

NOTE: Do not change any other parameters in the auto exposure tab.

6.2. Set-up the anesthesia system according to manufacturer's guidelines to deliver between

397 1.5% and 2% isoflurane to the anesthesia chamber and the imaging chamber.
398
399 6.3. Anesthetize metastasis-containing mice from step 4 by placing them in an anesthesia
400 chamber and delivering 1.5-2.5% isoflurane.
401
402 6.4. Prepare mice for bioluminescence imaging as follows.
403
404 6.4.1. Load a 1 mL syringe with D-luciferin (30 mg/mL in D-PBS) and then add a ½ inch 30-gauge
405 needle to the syringe and expel air bubbles.
406
407 6.4.2. Measure and record the mass of the mouse.
408
409 6.4.3. Restrain the mouse by pinching the scruff of their neck using the thumb and pointer fingers
410 and grasping the tail between the pinkie finger and the base of the hand. Invert the mouse at a
411 45-degree angle, with its head pointed downward.
412
413 6.4.4. Insert the needle, bevel side up, into the mouse's left side intraperitoneal (IP) space.
414 Confirm entry into the IP space by drawing back a small volume. There should not be color at the
415 base of the needle when drawing back in the IP space.
416
417 6.4.5. Inject the appropriate volume of D-luciferin for a dose of 150 mg/kg.
418
419 6.4.6. Immediately after D-luciferin administration, start a timer and place the mouse flat on its
420 back in the imaging device with its nose in the nose cone and ensure that 1.5-2.5% isoflurane is
421 being administered. Place dividers between each mouse if imaging multiple mice. Ensure mice
422 are positioned as flat as possible (i.e. not leaning to one side).
423
424 6.4.7. Click the **Luminescent** and **Photograph** boxes and then click **Acquire** in the **Acquisition**
425 **Control Panel**.
426
427 6.5. Continuously acquire bioluminescent images until the peak signal is achieved and use the
428 image with the peak bioluminescent signal for analysis.
429
430 6.6. After imaging, return the mouse to its cage and monitor for 15 minutes to ensure full
431 recovery.
432
433 6.7. Image 2-3 times weekly for the duration of the experiment.
434
435 7. **Quantification of the number and size of metastases**
436
437 NOTE: The length of time the metastases are allowed to grow should be determined for each cell
438 line and mouse strain, and will be influenced by the number of cells injected.
439
440 7.1. Euthanize the mice according to standard institutional guidelines.

7.2. Isolate and remove the lungs from each mouse and rinse in 1x PBS to remove excess blood.

7.3. Gently separate the lungs into lobes.

7.4. Acquire images of ZsGreen metastases in the lobes at 10x in bright field and fluorescence using a fluorescent stereoscope with a GFP wideband filter (excitation 470/40x).

NOTE: Maintain the same magnification and brightness for all samples. The magnification used may vary depending on the size, number, and brightness of metastases as well as the field of view for the microscope used.

7.5. Use image analysis software to quantify the size and number of metastases from the images.

NOTE: The protocol for image analysis is software dependent and could be optimized with tumors from step3. Alternatively, count the number of metastases in each lung manually using the fluorescent stereoscope. Protocol can be paused here and step 8 can be done at any point after all the in vivo images have been collected.

8. **Processing and analysis of the data from the images acquired with the in vivo live animal imaging device**

8.1. Open all image files for each mouse in the image software.

NOTE: Use the image with the peak bioluminescent signal for analysis

8.2. Ensure the units are in **Radiance** for bioluminescent data and **Efficiency** for fluorescent data by clicking the arrow at the top left of the image window and changing it to the appropriate unit.

8.3. Use the image from the last timepoint to create a region of interest (ROI) as follows.

8.3.1. Click **ROI Tools** in the **Tool Palette** window. Insert one ROI by clicking the arrow and selecting **1**.

8.3.2. Click the border of the ROI and move it over the chest of the mouse. Adjust the size of the ROI so it covers the chest of the mouse and does not exclude signal.

8.4. Click measure ROIs and copy or type the raw number into an excel sheet.

NOTE: For bioluminescent data select the total flux (photons/second), which is the sum of all the radiance in the ROI. Since metastases do not necessarily grow uniformly, the total flux is preferred over average radiance because it measures the sum of the metastatic burden. Similarly, for fluorescent data, the total efficiency % (emission light (photons/second)/excitation light (photons/second)) should be used instead of average efficiency.

485
486 8.5. Right click in the image file to copy the ROI used in step 8.3 and paste it into every image
487 file.
488
489 NOTE: When quantifying fluorescent images, quantify the same region on a mouse that was
490 imaged with no metastasis. Use this signal as the background signal and subtract it from each
491 fluorescent metastasis-containing mouse image acquired.
492
493 8.6. Move pasted ROIs over the same region selected in step 8.3.4 for each image and repeat
494 step 8.4.
495
496 8.7. Plot and analyze the raw data as follows (see **Supplemental Table 2**).
497
498 8.7.1. Do a $\log_{10}$ transformation of the raw data for each mouse using the indicated formula
499 (**Supplemental Table 2**) and plot as in **Figure 2D** and **Figure 4F**. The $\log_{10}$ transformation linearizes
500 the growth curve which tends to be geometric and minimizes heteroscedasticity.
501
502 8.7.2. Using linear regression, calculate the slope of the fitted line to the $\log_{10}$ transformed data
503 for each mouse plotted in step 8.7.1 (**Supplemental Table 2**). Refer to formula in supplemental
504 table 2 to fit the line and calculate the slope in one step.
505
506 8.7.3. Plot the numerical values of the slopes as in **Figure 2E** and **Figure 4G**. Use a Student's t-
507 test or one-way ANOVA (for more than 2 groups) on the slopes to determine statistical
508 significance.
509
510 **REPRESENTATIVE RESULTS:**
511 To demonstrate the above approach, we performed a proof of concept experiment in which a
512 critical replication factor, RPA3 was knocked down in a metastatic mouse mammary carcinoma
513 cell line (4T1[22]). While the protocol describes labeling the cells with both luciferase and
514 fluorescent proteins prior to genetic manipulation, we used a modified approach because THE
515 RNAi vectors also deliver ZsGreen (**Figure 2A**). First, 4T1 cells were stably transduced with a
516 lentiviral construct encoding firefly luciferase and hygromycin resistance (pHAGE-Luciferase-
517 IRES-Hygro). After hygromycin selection, a luciferase assay was performed to confirm stable
518 expression of the firefly luciferase (**Figure 2A**). Next, the 4T1-Luciferase cells were stably
519 transduced with retroviral vectors that express ZsGreen and either a control miR30-based shRNA,
520 or a miR30-based shRNA previously shown to effectively target mouse RPA3[23,24]. The cells were
521 then injected into the mice via the lateral tail vein and in vivo bioluminescent signal was
522 measured twice a week to monitor the metastatic burden (**Figure 2B,C**). The $\log_{10}$ transformed
523 signal for each mouse was plotted as metastatic burden over time (**Figure 2D**) and the slopes of
524 each plot were determined (**Figure 2E**). These data show the rate of change in metastatic burden
525 is significantly reduced with RPA3 knockdown compared to control cells. Although the differences
526 are striking, these data alone do not allow us to determine if the reduced metastatic burden is
527 the result of less metastases or due to slower growth of metastases. Therefore, the ZsGreen-
528 labeled metastases in the lungs were also analyzed at the end of the experiment. Mice injected

529 with RPA3 knockdown cells had almost no metastases in the lungs, whereas the control mice had
530 numerous large metastases (**Figure 3**). Furthermore, the metastases that did form from RPA3
531 knockdown cells were clearly smaller than control 4T1 metastases (**Figure 3A**). Consistent with
532 our manual counts (**Figure 3B**), image analysis software counted significantly less metastases in
533 the RPA3 knockdown mice (**Figure 3C**). Additionally, the total metastatic burden in the lungs (sum
534 of the areas of each metastasis in millimeters) was also drastically reduced by RPA3 knockdown
535 (**Figure 3D**). Finally, the size of the individual metastases that formed in the RPA3 knockdown
536 mice were generally much smaller than those in the control mice (**Figure 3E**). In addition to the
537 large metastases in the control mice, we did observe numerous small metastases as well, but
538 cannot determine if these are tumor cells that seeded the lung and did not grow or if they are
539 tumor cells shed from one of the larger metastases that re-seeded the lung in a new location
540 (**Figure 3E**). Collectively these data show that RPA3 is required for metastasis formation by 4T1
541 cells. These findings were expected because our previous work showed that RPA3 knock down
542 cells had significantly reduced ability to form metastases in the lungs following tail vein
543 injection[16]. However, this experiment demonstrates how the use live animal imaging and
544 fluorescent quantification of metastasis number and size can be used to determine if changes in
545 metastatic burden are due to differences in metastatic colonization or growth.
546
547 To demonstrate how this approach can be used to answer a more biologically relevant question,
548 we asked if YAP and TAZ are required for metastatic colonization and subsequent growth in this
549 syngeneic model of breast cancer. The expression and activity of YAP or TAZ are increased in
550 many cancers compared to normal tissue and this is predictive of poor patient outcome[25-29].
551 Additionally, several studies have implicated YAP, TAZ, or TEADs, the critical YAP/TAZ-binding
552 partners, in metastasis[15,30-52]. Given this data we used our approach to test if YAP and TAZ are
553 required for metastasis formation and growth. For this, we use a retroviral vector expressing
554 tandem miR30-based shRNAs targeting both YAP and TAZ. As shown, this tandem shRNA
555 effectively reduces YAP and TAZ protein expression and transcriptional activity in 4T1 cells (**Figure
556 4A,4B**). 4T1-Luciferase cells were stably transduced with a ZsGreen-expressing version of this
557 tandem YAP/TAZ shRNA vector or a control miR30-based shRNA (**Figure 4C**) and then assayed by
558 tail vein injections in syngeneic BALB/c mice. As shown in **Figure 4**, the rate at which metastatic
559 burden increased was significantly faster in the mice injected with control cells compared to the
560 mice injected with YAP/TAZ knockdown cells (**Figure 4D-F**). Significantly fewer metastases
561 formed in the mice injected with YAP/TAZ knockdown cells compared to mice with control cells
562 whether counted manually (**Figure 5A,5B**) or using the image analysis software (**Figure 5C**). Not
563 only did many more metastases form in the control mice, but they were generally larger (**Figure
564 5E**). Consistently, the metastatic burden in the lungs (total metastasis area in mm) was also
565 drastically reduced by YAP/TAZ knockdown (**Figure 5D**). It is important to note that when the
566 metastases are large and close together, the software may be unable to differentiate distinct
567 metastases. This was the case for a few metastases in control mice (mouse 3 and mouse 7). Thus,
568 it is important to check the output of the image analysis software to ensure it is accurately
569 measuring the area of single tumors. This is also why it is important to optimize the number of
570 cells being injected and the length of the experiment. Collectively, these data show that YAP and
571 TAZ are required to sustain the rate at which metastatic burden increases in a syngeneic murine
572 model of metastatic breast cancer and that this is due to the inability of metastases to form and

573　reduced growth of the few metastases that did form.

574

575　**FIGURE AND TABLE LEGENDS:**

576

577　**Figure 1. Schematic of the protocol.** All necessary viruses are first packaged in HEK-293FT cells.
578　The desired cells for the study are then simultaneously infected with luciferase and fluorescent
579　viruses that each express a unique mammalian drug selection gene. Infected cells are then
580　expanded in the appropriate media containing both drugs to select for stably transduced cells
581　expressing both luciferase and the florescent protein. Expression of both labels is confirmed as
582　described in the protocol. The labeled cells are then transduced with a third virus a containing
583　genetic manipulation (miR30 shRNA) and a third unique drug selection gene. After selection with
584　the third drug, the cells are injected into the mice via the lateral tail vein. Metastatic burden is
585　monitored in the mice throughout the experiment with an in vivo live animal imaging system. At
586　the end of the experiment, mice are euthanized, and images of the whole lungs are taken using
587　a fluorescent dissecting microscope, and then used to measure the number and size of
588　metastases.

589

590　**Figure 2. Luciferase-based in vivo live animal imaging shows that RPA3 knockdown reduces**
591　**breast cancer metastatic burden.** (**A**) Schematic showing how the cells were generated for this
592　in vivo study. 4T1 cells were stably transduced with a lentivirus encoding luciferase and
593　hygromycin resistance. Infected cells were selected with 600 μg/mL of hygromycin B for one
594　week and then luciferase activity was measured in parental or 4T1-luciferase cells using a
595　luciferase reporter kit and plate reader (n=1 experiment with replicate wells averaged). 4T1-
596　Luciferase cells were then infected with retrovirus that deliver ZsGreen and miR30 shRNAs
597　targeting either mCherry (control) or mRPA3. Puromycin selection (2.5 μg/mL) for 3 days was
598　used to select for stable integration of the virus. (**B-E**) 4T1-luciferase cells stably expressing
599　ZsGreen and control (sh-mCherry) or mRPA3 (sh-mRPA3-431) shRNAs were injected into mice
600　and imaged for bioluminescence on the indicated days as described in the protocol. (**B&C**)
601　Bioluminescent images for a representative mouse of each group on the indicated day post
602　injection (**D**) Plot of the $\log_{10}$ transformed luciferase signal measured for each mouse over the
603　course of the experiment. (**E**) Scatter plot with mean (solid line) for the slopes of each mouse in
604　D (n=6 for sh-control and 8 for sh-mRPA3-431). Statistical significance was tested using a
605　Student's *t* test; *p ≤ 0.05.

606

607　**Figure 3. Quantification of fluorescent metastases reveals that RPA3 knockdown prevents**
608　**metastatic colonization and subsequent growth of breast cancer cells.** (**A**) Fluorescent (left) and
609　brightfield (right) images of representative lobes from each mouse injected in Figure 2 21 days
610　after injection. Asterisks (*) indicated green autofluorescent bronchi. (**C-E**) Image analysis
611　software (see **Table of Materials**) was used to identify and measure objects using an intensity
612　threshold of 25 to 100 and a size threshold of 0.01 mm^2 to infinity. (**B&C**) Scatter plot with the
613　Mean (solid bar) of the total number of metastases in the lungs of each mouse when counted (**B**)
614　by image analysis software (**C**). (**D**) The total area (mm) of lung that was measured with image
615　analysis software is plotted as metastatic burden with the Mean indicated by a solid bar. (**E**) The
616　size of each metastasis is plotted for every mouse. Control mice are indicated by the blue dots

617 and mRPA3 knockdown mice by the red dots. Note, the scale bar is separated at 1 mm to make
618 it easier to visualize the size and number of small metastases (n=6 sh-control, 8 sh-mRPA3-431).
619 Statistical significance was tested using a Student's t test; $p = 0.06$; ** p $\leq$ 0.01.

620

621 **Figure 4. YAP/TAZ knockdown reduces breast cancer metastatic burden. (A&B)** 4T1 cells stably
622 expressing miR30-based control (mCherry) or tandem YAP/TAZ shRNAs (sh-mYAP1/mTAZ6) were
623 analyzed by Western blot analysis (**A**) or transfected with a YAP/TAZ-TEAD luciferase reporter
624 construct and assayed for YAP/TAZ-TEAD transcriptional activity as described previously[15,16] (**B**)
625 (n = 5 for control and 4 for YAP1/TAZ6). (**C**) Schematic showing how the cells were generated for
626 the in vivo study. 4T1-Luciferase cells were infected with retroviruses that deliver ZsGreen and
627 either a miR30 shRNA targeting mCherry (control) or tandem miR30 shRNAs targeting both mYAP
628 and mTAZ. Infected cells were selected in Puromycin (2.5 µg/mL) for 3 days. 4T1-luciferase cells
629 stably expressing ZsGreen and control (sh-mCherry) or YAP/TAZ (sh-mYAP1/mTAZ1) shRNAs
630 were then injected into mice and imaged for bioluminescence by on the injected days. (**D&E**)
631 Bioluminescent images for a representative mouse of each group on the indicated day post
632 injection. (**F**) Plot of the $\log_{10}$ transformed luciferase signal measured for each mouse over the
633 course of the experiment. (**G**) Scatter plot with Mean (solid bar) for the slopes of each mouse in
634 **F** (n = 7 for sh-control and 8 for sh-mRPA3-431). Mean is indicated by a solid line. Statistical
635 significance was tested using a Student's t test; $p = 0.06$; #, $p \leq 0.01$; ***.

636

637 **Figure 5. YAP and TAZ are required for metastatic breast cancer cells to colonize the lungs. (A)**
638 Fluorescent (left) and brightfield (right) images of representative lobes from each mouse injected
639 in **Figure 4** 21 days after injection. (**C-E**) Images were processed with image analysis software as
640 described in **Figure 3**. (**B&C**) Scatter plot with the Mean (solid bar) of the total number of
641 metastases in the lungs of each mouse when counted manually (**B**) or by image analysis software
642 (**C**). (**D**) The total area of all metastases (mm) was measured with image analysis software and
643 plotted as metastatic burden with the Mean (solid bar). (**E**) The size of each metastasis is plotted
644 for every mouse. Control mice are indicated by the blue dots and sh-mYAP1/mTAZ6 knockdown
645 mice by the red dots. Note, the scale bar is separated at 1 mm to better visualize the size and
646 number of small metastases (n = 7 sh-control, 8 sh-mYA1/mTAZ6). Mean is indicated by a solid
647 line. Statistical significance was tested using a Student's t test; *p $\leq$ 0.05, **, $p \leq$ 0.01; **.

648

649 **Supplemental Table 1. Table of vectors.** All vectors used are listed and new vectors are
650 described. Standard molecular biology techniques were used to clone new vectors and
651 sequences for newly described 97-mer shRNA are included. Citations refer to: [1][53], [2][16], [3][54]

652

653 **Supplemental Table 2. Example of in vivo live animal imaging data processing and analysis.**
654 Spreadsheet demonstrating how the raw data from the in vivo live animal images is converted
655 for analysis as described in steps 6.7 and 6.8. Raw data acquired from the in vivo live animal
656 imaging transformed using a $\log_{10}$ transformation. The rate of change in metastatic burden is
657 calculated for each mouse by calculating the slope generated by the $\log_{10}$ transformed data.
658 Examples include luciferase analysis from **Figure 2**. The columns are color-coded to indicate
659 which data was used to generate each slope value and the formulas are imbedded in the
660 spreadsheet. Double clicking the well will reveal the formula used to process the data.

661
662 **DISCUSSION:**

663

664 **Critical steps of the method**
665 It is critical to optimize the number of cells injected (step 3) for a given cell line and mouse strain
666 as this can greatly influence the number of metastases that form and the length of the
667 experiment. If too many cells are injected or the metastases grow for too long, the metastases
668 may be difficult to count making the effects of the genetic manipulation difficult to assess.
669 However, if too few cells are injected, few or no metastases may form. Thus, a preliminary
670 experiment should be done using different numbers of cells to determine the optimal number
671 and the length of time that the metastases grow. To ensure consistent numbers of metastases
672 within a group, it is important inject equal numbers of viable cells into each mouse. Since cells
673 can settle in both the tube and syringe, cells should be gently resuspended prior to loading the
674 syringe, and cell suspensions should not be left in the syringe for too long (step 4.3.2). Cell
675 viability decreases the longer the cells are in suspension, so the amount of time between
676 trypsinization and injection of the cells should be no more than one hour (step 4.2.5). Air bubbles
677 and large clumps of cells should not be injected since these can cause emboli that kill the mouse.
678 In addition, drawing cells up through the needle can shear them, so the syringe should be loaded
679 without the needle. To confirm that a relatively equal number of cells was injected, in vivo live
680 animal images can be taken shortly after the injection (**Figure 2B, Figure 4D**).

681

682 Accurate and consistent quantification of the bioluminescent signal is important and dependent
683 upon the cells taking up and metabolizing the D-luciferin. This can be influenced by many
684 variables including, the dose of D-luciferin, timing of injection, mouse's body temperature, how
685 anesthetized the mouse is when injected, and how a mouse is positioned in the anesthesia
686 chamber prior to imaging. Therefore, it is critical to keep these steps consistent for all mice and
687 imaging sessions. We used a heating pad to maintain consistent mouse body temperature while
688 in the anesthesia chamber. Since the signal must penetrate the tissue for both bioluminescent
689 and fluorescent detection, it is also critical to keep the mouse position consistent for each image
690 (flat on its back works best for imaging of the lungs). Quantification of fluorescent images from
691 the in vivo live animal imaging should always be done using the efficiency % units as this allows
692 for appropriate comparison between images. Likewise, total flux (photons/second) should always
693 be used when quantifying bioluminescent images. For analysis of the metastatic burden, the $\log_{10}$
694 transformation converts the growth curve (before maximum signal is reached) into a linear plot,
695 which was necessary for the slope analysis.

696

697 **Modifications, and troubleshooting of the method**
698 In the presented protocol a population of cells is first stably transduced with a fluorescent protein
699 and luciferase, then that population is transduced with either a control vector or a vector
700 targeting the gene of interest. This ensures that both cell populations have similar fluorescent
701 protein and luciferase expression. However, as an alternative, viral vectors that simultaneously
702 deliver two of these components could be utilized. Indeed, in the representative experiments we
703 used ZsGreen expressing retroviral vectors to express the shRNAs in 4T1-luciferase cells. It is
704 recommended that the expression of the luciferase and the fluorescent protein be assayed in all

705 cell groups after the gene of interest is altered. Different levels of expression between groups
706 can complicate the interpretation of the data, so it is best if the different groups have similar
707 expression of both the fluorescent protein and luciferase. Additionally, red blood cells can be
708 autofluorescent and may make it difficult to visualize the fluorescent metastases in the lungs. If
709 this is the case, red blood cells can be cleared from the lungs by PBS perfusion during euthanasia
710 to reduce autofluorescent background (appropriate euthanasia techniques and guidelines should
711 be followed). Although the differences between control and knockdown groups in our
712 representative experiments are dramatic, the inherent mouse-to-mouse variability that often
713 exists in in vivo metastasis assays is evident in the control mice (**Figure 3B** and **Figure 5B**). When
714 this variability is high, it can make it difficult to determine the magnitude of the knockdown
715 effect. An alternative approach that could be used to reduce this variability is to label the control
716 cells and knockdown cells with distinct fluorescent proteins and distinct luciferase enzymes and
717 then mix the two populations in equal numbers and inject the mixture. For example, control cells
718 stably expressing tomato and renilla luciferase could be mixed with knockdown cells expressing
719 ZsGreen and firefly luciferase. In vivo live animal imaging devices can distinguish renilla luciferase
720 from firefly luciferase, and tomato from ZsGreen, so either fluorescence or luminescence can be
721 used to independently quantify each cell population. Indeed, dual luciferase imaging of 4T1 cells
722 growing as primary tumors in live animals has been demonstrated using an in vivo live animal
723 imaging device[4]. However, it is important to note that there may be overlap in fluorescent signal,
724 thus a spectral unmixing step (see manufacturers guidelines) should be included in this approach.
725 Additionally, the renilla luciferase and firefly luciferase should be imaged separately with an
726 adequate time delay that allows for the first luciferase signal to no longer be detectable prior to
727 imaging the second. Use of distinct fluorophores still enables the number and size of metastasis
728 in the lungs to be quantified[16]. To test metastatic colonization and growth in other organs besides
729 the lungs this protocol can be modified and used for intracardiac and portal vein injections[9,10].
730
731 **Limitations of the method**
732 Using an in vivo live animal imaging device to acquire real time metastatic burden in conjunction
733 with fluorescently labeled cancer cells provides a powerful method to assay metastatic
734 colonization and subsequent growth; however, there are limitations of this approach. Some
735 genes may be required for innate cell proliferation rather than specific roles in metastasis. In vitro
736 cell proliferation assays could be done prior to the in vivo experiment to determine if the gene
737 disrupts in vitro growth. When imaging a live animal, the bioluminescent or fluorescent signal
738 from metastases must be strong enough to pass through the tissue. Additionally, the optical
739 properties (i.e., absorption and scattering) of the tissue also influence detection[55]. The excitation
740 light source must be able to pass through tissue to excite fluorescently labeled cancer cells and
741 bioluminescence has a larger dynamic range than fluorescence. Thus, although fluorescence can
742 be used for live animal imaging, bioluminescence is preferred for detecting signal in internal
743 organs. In addition, some immunocompetent mouse strains may reject cells expressing
744 fluorescent proteins. Indeed, we found that cells expressing tomato, GFP, or mCherry were
745 rejected or down regulated the fluorophore when growing in BALB/c mice (data not shown
746 and[15]). However, as demonstrated here (**Figure 3** and **Figure 5**) and previously[15,16], ZsGreen-
747 labeled cells are detectable in these mice. In cases where the fluorescent protein expression
748 becomes undetectable, another way to quantify the relative metastatic colonization is to use

749 qPCR to quantify either the fluorescent gene or another gene in the integrated viral vector[15].
750 Although an in vivo live animal imaging device allows you to detect changes in metastatic burden,
751 it does not allow one to determine if these changes are due to altered size or number of
752 metastases. It also does not provide spatial information about the location of the metastases.
753 Furthermore, the strength of the signal can be influenced by how deep in the tissue it is.
754
755 **The significance of the method and potential future applications**
756 There are many ways in which this approach can be modified to gain more or different
757 information. A variety of cancer cell lines including human cancer cell lines or patient derived
758 xenografts could be used in this assay. Other mouse models could also be used, including
759 transgenic or knockout mice designed to test how targeting proteins made by stromal cells
760 influences the metastatic colonization and growth of the injected cancer cells. If there are
761 multiple candidate genes to be tested, this approach can be multiplexed because in vivo live
762 animal imaging devices can detect and distinguish a wide range of fluorophores. This would
763 reduce the number of mice required and increase the number of targets that can be tested. In
764 vivo live animal imaging can also be combined with X-ray or CT[9] imaging to provide a great deal
765 more spatial information about the location of the metastases. Lastly, this approach can be
766 modified to assay more specific steps within the metastatic colonization cascade. For example,
767 the steps involved in tumor cell seeding (intravascular survival, extravasation, and post
768 extravasation survival) can be distinguished by quantifying the number of tumor cells in the lungs
769 at several time points within the first 3 days following injection (such as done here[16]). In this case,
770 the lungs can also be stained with vascular markers and imaged ex vivo to determine the
771 percentage of cancer cells that have extravasated at each time point[56,57].
772
773 In summary, the use of real-time in vivo live animal imaging of fluorescent and luminescent
774 cancer cells following tail vein injection enables a more detailed analysis of how a candidate gene
775 or genes influences metastatic colonization and subsequent growth. This approach is faster and
776 less expensive than autochthonous mouse models and avoids some of the caveats of
777 spontaneous metastasis models. The use of both fluorescence and luminescence as a means to
778 detect and quantify metastases gives researchers independent readouts that improve confidence
779 in the results and allow for flexibility in the experimental design. The use of fluorescence to
780 quantify metastasis size and number avoids the need for time-consuming and potentially costly
781 histological processing and analysis, and allows for additional use of the whole tissues. The
782 protocol can be used with a number of different techniques to manipulate the expression or
783 function of the candidate gene, such as RNAi, transgene expression, or CRISPR/Cas-mediated
784 editing, and can also be used to test small molecules, function blocking antibodies, or other
785 potential therapeutic compounds. As mentioned above, several simple modifications can be
786 made to enhance the assay and provide additional information. This approach is an ideal way to
787 identify and test pro-metastatic genes that have therapeutic potential for the treatment of
788 cancer.
789

797 **DISCLOSURES:**
798 The authors have nothing to disclose.
799

800 **REFERENCES**:

801 1   Ferlay, J. S. I. et al. *GLOBOCAN 2012 v1.0, Cancer Incidence and Mortality Worldwide: IARC*
802 *CancerBase No. 11 [Internet].* < http://globocan.iarc.fr> (2013).
803 2   Gupta, G. P., Massague, J. Cancer metastasis: building a framework. *Cell.* **127** (4), 679-695
804 (2006).
805 3   Chaffer, C. L., Weinberg, R. A. A perspective on cancer cell metastasis. *Science.* **331** (6024),
806 1559-1564 (2011).
807 4   Wendt, M. K., Molter, J., Flask, C. A., Schiemann, W. P. In vivo dual substrate
808 bioluminescent imaging. *Journal of Visualized Experiments.* (56) (2011).
809 5   Moret, R. et al. Patient-derived Orthotopic Xenograft Models for Human Urothelial Cell
810 Carcinoma and Colorectal Cancer Tumor Growth and Spontaneous Metastasis. *Journal of*
811 *Visualized Experiments.* (147) (2019).
812 6   Lizardo, M. M., Sorensen, P. H. Practical Considerations in Studying Metastatic Lung
813 Colonization in Osteosarcoma Using the Pulmonary Metastasis Assay. *Journal of Visualized*
814 *Experiments.* (133) (2018).
815 7   Mohanty, S., Xu, L. Experimental metastasis assay. *Journal of Visualized Experiments.* (42)
816 (2010).
817 8   Welch, D. R. Technical considerations for studying cancer metastasis in vivo. *Clinical and*
818 *Experimental Metastasis.* **15** (3), 272-306 (1997).
819 9   Lim, E. et al. Monitoring tumor metastases and osteolytic lesions with bioluminescence
820 and micro CT imaging. *Journal of Visualized Experiments.* (50) (2011).
821 10   Goddard, E. T., Fischer, J., Schedin, P. A Portal Vein Injection Model to Study Liver
822 Metastasis of Breast Cancer. *Journal of Visualized Experiments.* (118) (2016).
823 11   Cordero, A. B., Kwon, Y., Hua, X., Godwin, A. K. In vivo imaging and therapeutic treatments
824 in an orthotopic mouse model of ovarian cancer. *Journal of Visualized Experiments.* (42) (2010).
825 12   Ozawa, T., James, C. D. Establishing intracranial brain tumor xenografts with subsequent
826 analysis of tumor growth and response to therapy using bioluminescence imaging. *Journal of*
827 *Visualized Experiments.* (41) (2010).
828 13   Lim, E., Modi, K. D., Kim, J. In vivo bioluminescent imaging of mammary tumors using IVIS
829 spectrum. *Journal of Visualized Experiments.* (26) (2009).
830 14   Oshima, G. et al. Advanced Animal Model of Colorectal Metastasis in Liver: Imaging
831 Techniques and Properties of Metastatic Clones. *Journal of Visualized Experiments.* (117) (2016).
832 15   Lamar, J. M. et al. SRC tyrosine kinase activates the YAP/TAZ axis and thereby drives tumor
833 growth and metastasis. *Journal of Biological Chemistry.* **294** (7), 2302-2317 (2019).
834 16   Lamar, J. M. et al. The Hippo pathway target, YAP, promotes metastasis through its TEAD-
835 interaction domain. *Proceedings of the National Academy of Sciences U S A.* **109** (37), E2441-2450
836 (2012).

837   17   Warren, J. S. A., Xiao, Y., Lamar, J. M. YAP/TAZ Activation as a Target for Treating
838   Metastatic Cancer. *Cancers (Basel).* **10** (4) (2018).
839   18   Janse van Rensburg, H. J., Yang, X. The roles of the Hippo pathway in cancer metastasis.
840   *Cell Signal.* **28** (11), 1761-1772 (2016).
841   19   Harvey, K. F., Pfleger, C. M., Hariharan, I. K. The Drosophila Mst ortholog, hippo, restricts
842   growth and cell proliferation and promotes apoptosis. *Cell.* **114** (4), 457-467 (2003).
843   20   Journal of Visualized Experiments Science Education Database. *Basic Methods in Cellular*
844   *and Molecular Biology.* **The Western Blot** (2019).
845   21   Wong, W., Farr, R., Joglekar, M., Januszewski, A., Hardikar, A. Probe-based Real-time PCR
846   Approaches for Quantitative Measurement of microRNAs. *Journal of Visualized Experiments.* (98)
847   (2015).
848   22   Aslakson, C. J., Miller, F. R. Selective events in the metastatic process defined by analysis
849   of the sequential dissemination of subpopulations of a mouse mammary tumor. *Cancer*
850   *Ressearch.* **52** (6), 1399-1405 (1992).
851   23   Fellmann, C. et al. Functional identification of optimized RNAi triggers using a massively
852   parallel sensor assay. *Molecular Cell.* **41** (6), 733-746 (2011).
853   24   Reticker-Flynn, N. E. et al. A combinatorial extracellular matrix platform identifies cell-
854   extracellular matrix interactions that correlate with metastasis. *Nature Communications.* **3**, 1122
855   (2012).
856   25   Sun, Z. et al. Prognostic Value of Yes-Associated Protein 1 (YAP1) in Various Cancers: A
857   Meta-Analysis. *Public Library of Science One.* **10** (8), e0135119 (2015).
858   26   Feng, J., Ren, P., Gou, J., Li, Z. Prognostic significance of TAZ expression in various cancers:
859   a meta-analysis. *Onco Targets and Therapy.* **9**, 5235-5244 (2016).
860   27   Ge, L. et al. Yes-associated protein expression in head and neck squamous cell carcinoma
861   nodal metastasis. *Public Library of Science One.* **6** (11), e27529 (2011).
862   28   Zhang, X. et al. The Hippo pathway transcriptional co-activator, YAP, is an ovarian cancer
863   oncogene. *Oncogene.* **30** (25), 2810-2822 (2011).
864   29   Vlug, E. J. et al. Nuclear localization of the transcriptional coactivator YAP is associated
865   with invasive lobular breast cancer. *Cellular Oncology (Dordrecht).* **36** (5), 375-384 (2013).
866   30   Kim, T. et al. MRTF potentiates TEAD-YAP transcriptional activity causing metastasis.
867   *European Molecular Biology Organization Journal.* **36** (4), 520-535 (2017).
868   31   Nallet-Staub, F. et al. Pro-invasive activity of the Hippo pathway effectors YAP and TAZ in
869   cutaneous melanoma. *Journal of Investigative Dermatology.* **134** (1), 123-132 (2014).
870   32   Hsu, Y. L. et al. Angiomotin decreases lung cancer progression by sequestering oncogenic
871   YAP/TAZ and decreasing Cyr61 expression. *Oncogene.* **34** (31), 4056-4068 (2015).
872   33   Lau, A. N. et al. Tumor-propagating cells and Yap/Taz activity contribute to lung tumor
873   progression and metastasis. *European Molecular Biology Organization Journal.* **33** (5), 468-481
874   (2014).
875   34   Gu, J. J. et al. Inactivation of ABL kinases suppresses non-small cell lung cancer metastasis.
876   *Journal of Clinical Investigation Insight.* **1** (21), e89647 (2016).
877   35   Diepenbruck, M. et al. Tead2 expression levels control the subcellular distribution of Yap
878   and Taz, zyxin expression and epithelial-mesenchymal transition. *Journal of Cell Science.* **127** (Pt
879   7), 1523-1536 (2014).
880   36   Han, S. et al. Suppression of miR-16 promotes tumor growth and metastasis through

881   reversely regulating YAP1 in human cholangiocarcinoma. *Oncotarget.* **8** (34), 56635-56650
882   (2017).

883   37   Yin, K. et al. Netrin-1 promotes metastasis of gastric cancer by regulating YAP activity.
884   *Biochemical Biophysical Research Communications.* **496** (1), 76-82 (2018).

885   38   Guo, L. et al. Knockdown of TAZ modifies triple-negative breast cancer cell sensitivity to
886   EGFR inhibitors by regulating YAP expression. *Oncology Reports.* **36** (2), 729-736 (2016).

887   39   Liu, Y. N. et al. Loss of Androgen-Regulated MicroRNA 1 Activates SRC and Promotes
888   Prostate Cancer Bone Metastasis. *Molecular and Cellular Biology.* **35** (11), 1940-1951 (2015).

889   40   Bartucci, M. et al. TAZ is required for metastatic activity and chemoresistance of breast
890   cancer stem cells. *Oncogene.* **34** (6), 681-690 (2015).

891   41   Wang, T. et al. YAP promotes breast cancer metastasis by repressing growth
892   differentiation factor-15. *Biochimica et Biophysica Acta Molecular Basis of Disease.* **1864** (5 Pt A),
893   1744-1753 (2018).

894   42   Wang, J., Rouse, C., Jasper, J. S., Pendergast, A. M. ABL kinases promote breast cancer
895   osteolytic metastasis by modulating tumor-bone interactions through TAZ and STAT5 signaling.
896   *Science Signaling.* **9** (413) (2016).

897   43   Sun, S., Irvine, K. D. Cellular Organization and Cytoskeletal Regulation of the Hippo
898   Signaling Network. *Trends in Cell Biology.* **26** (9), 694-704 (2016).

899   44   Sharif, G. M. et al. Cell growth density modulates cancer cell vascular invasion via Hippo
900   pathway activity and CXCR2 signaling. *Oncogene.* **34** (48), 5879-5889 (2015).

901   45   Li, C. et al. A ROR1-HER3-lncRNA signalling axis modulates the Hippo-YAP pathway to
902   regulate bone metastasis. *Nature Cell Biology.* **19** (2), 106-119 (2017).

903   46   Pei, T. et al. YAP is a critical oncogene in human cholangiocarcinoma. *Oncotarget.* **6** (19),
904   17206-17220 (2015).

905   47   Qiao, Y. et al. YAP Regulates Actin Dynamics through ARHGAP29 and Promotes
906   Metastasis. *Cell Reports.* **19** (8), 1495-1502 (2017).

907   48   Zhou, W., Li, X., Premont, R. T. Expanding functions of GIT Arf GTPase-activating proteins,
908   PIX Rho guanine nucleotide exchange factors and GIT-PIX complexes. *Journal of Cell Science.* **129**
909   (10), 1963-1974 (2016).

910   49   Haemmerle, M. et al. Platelets reduce anoikis and promote metastasis by activating YAP1
911   signaling. *Nature Communcations.* **8** (1), 310 (2017).

912   50   Liu, Y. et al. Increased TEAD4 expression and nuclear localization in colorectal cancer
913   promote epithelial-mesenchymal transition and metastasis in a YAP-independent manner.
914   *Oncogene.* **35** (21), 2789-2800 (2016).

915   51   Hiemer, S. E. et al. A YAP/TAZ-Regulated Molecular Signature Is Associated with Oral
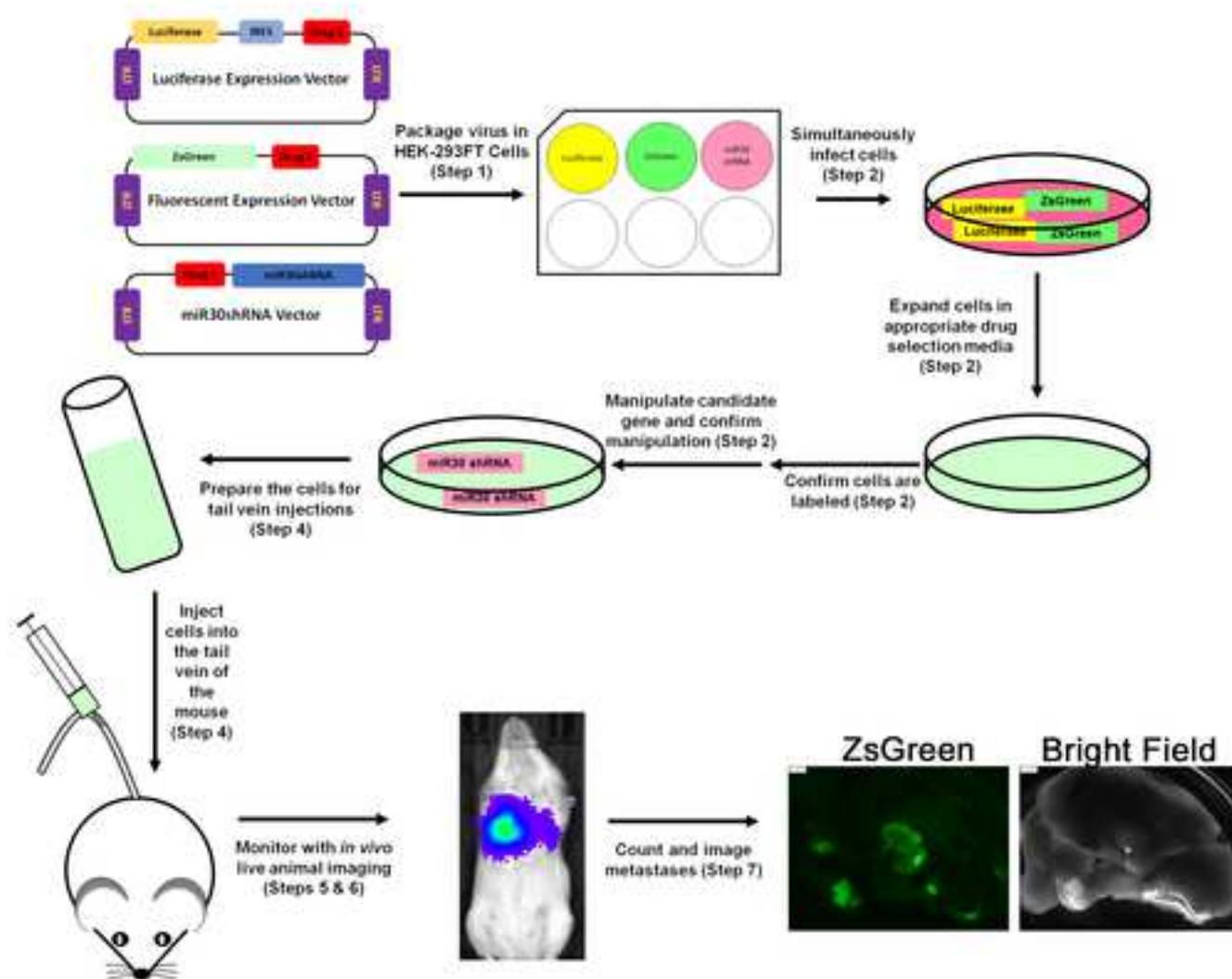916   Squamous Cell Carcinoma. *Molecular Cancer Research.* **13** (6), 957-968 (2015).

917   52   Lee, H. J. et al. Fluid shear stress activates YAP1 to promote cancer cell motility. *Nature
918   Communications.* **8**, 14122 (2017).

919   53   Naviaux, R. K., Costanzi, E., Haas, M., Verma, I. M. The pCL vector system: rapid production
920   of helper-free, high-titer, recombinant retroviruses. *Journal of Virology.* **70** (8), 5701-5705 (1996).
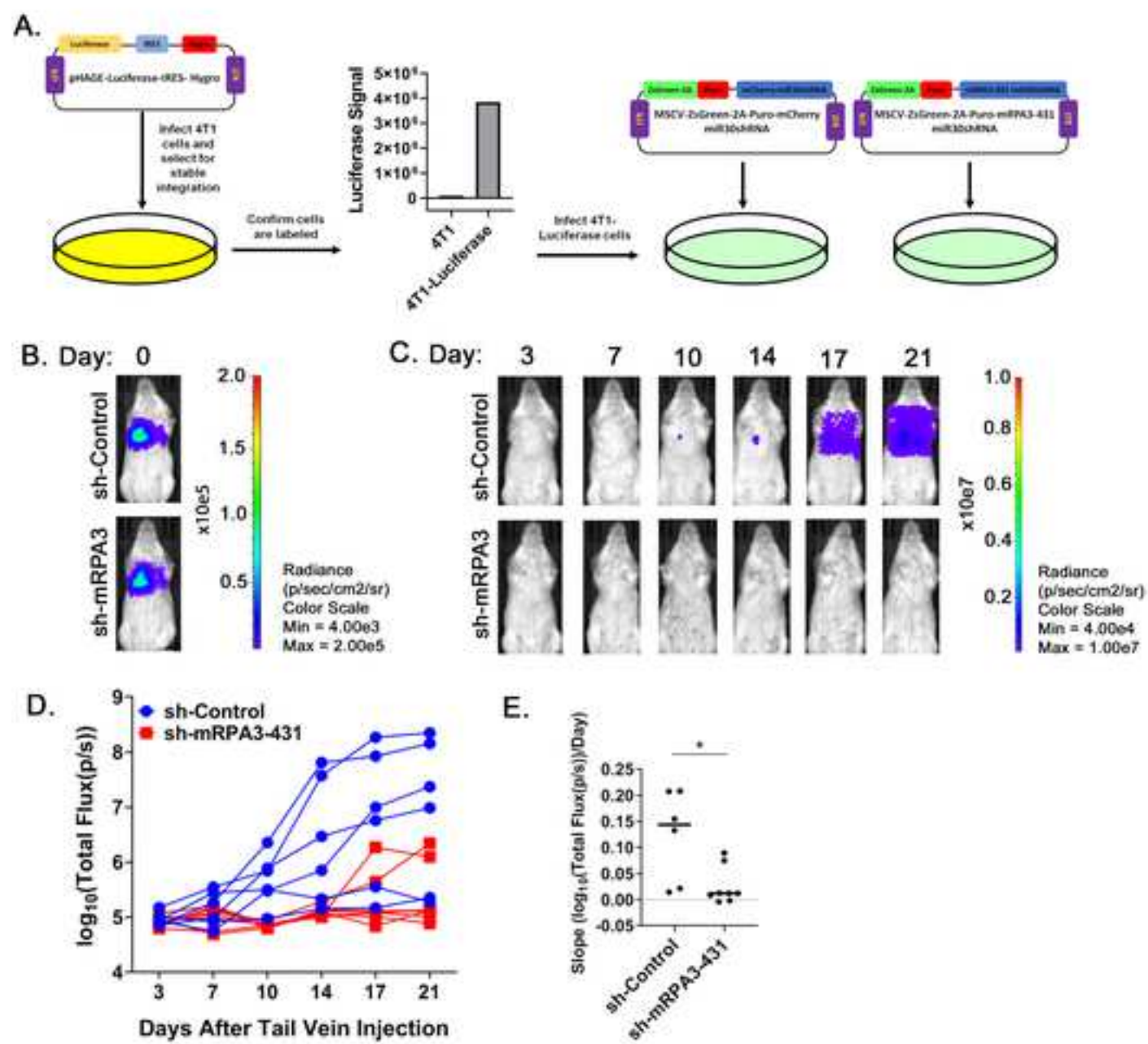
921   54   Mahoney, W. M., Jr., Hong, J. H., Yaffe, M. B., Farrance, I. K. The transcriptional co-
922   activator TAZ interacts differentially with transcriptional enhancer factor-1 (TEF-1) family
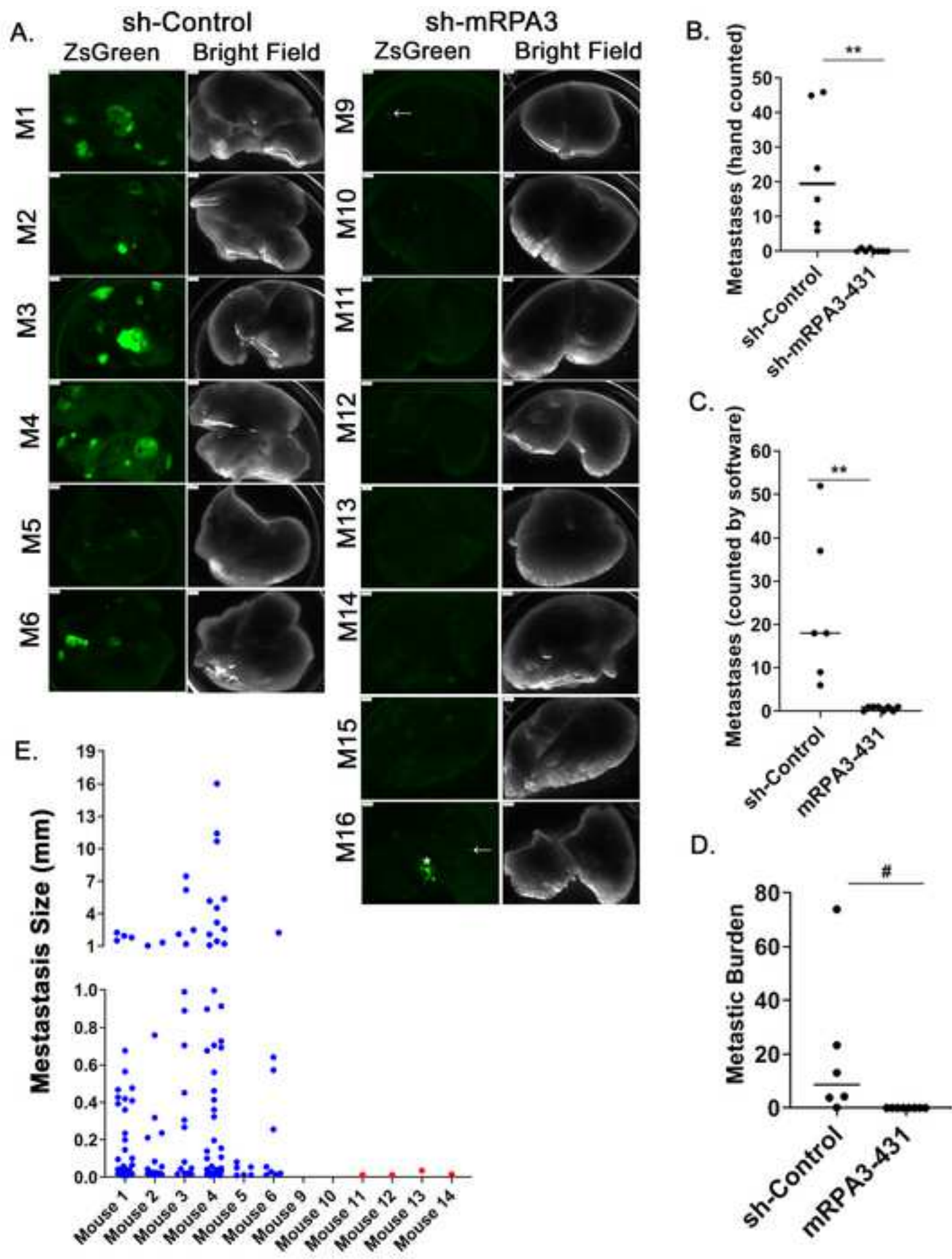923   members. *Biochemical Journal.* **388** (Pt 1), 217-225 (2005).

924   55   Zhao, H. et al. Emission spectra of bioluminescent reporters and interaction with
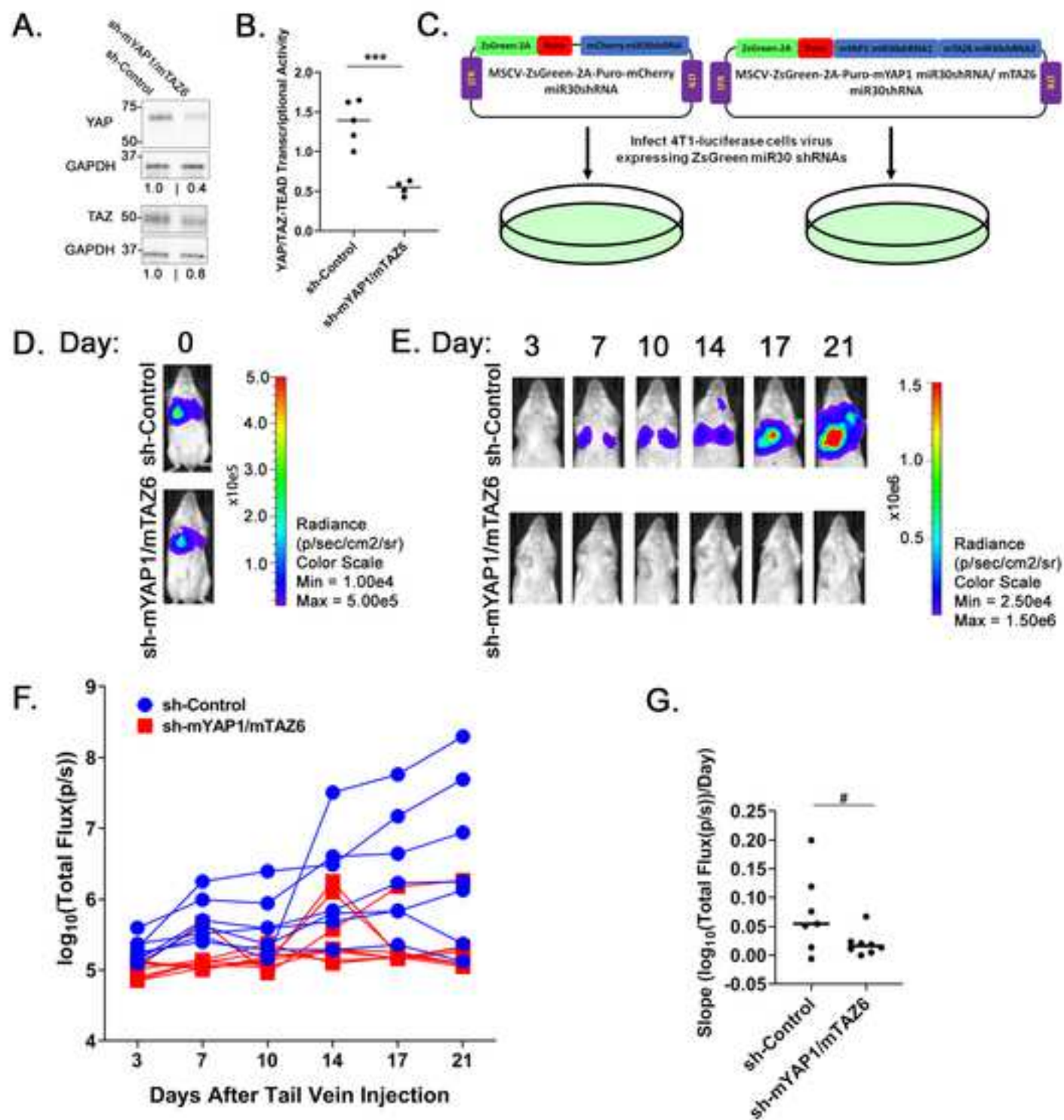
925 mammalian tissue determine the sensitivity of detection in vivo. *Journal of Biomedical Optics.* **10**
926 (4), 41210 (2005).
927 56   Chen, M. B., Lamar, J. M., Li, R., Hynes, R. O., Kamm, R. D. Elucidation of the Roles of
928 Tumor Integrin beta1 in the Extravasation Stage of the Metastasis Cascade. *Cancer Resesearch.*
929 **76** (9), 2513-2524 (2016).
930 57   Labelle, M., Begum, S., Hynes, R. O. Direct signaling between platelets and cancer cells
931 induces an epithelial-mesenchymal-like transition and promotes metastasis. *Cancer Cell.* **20** (5),
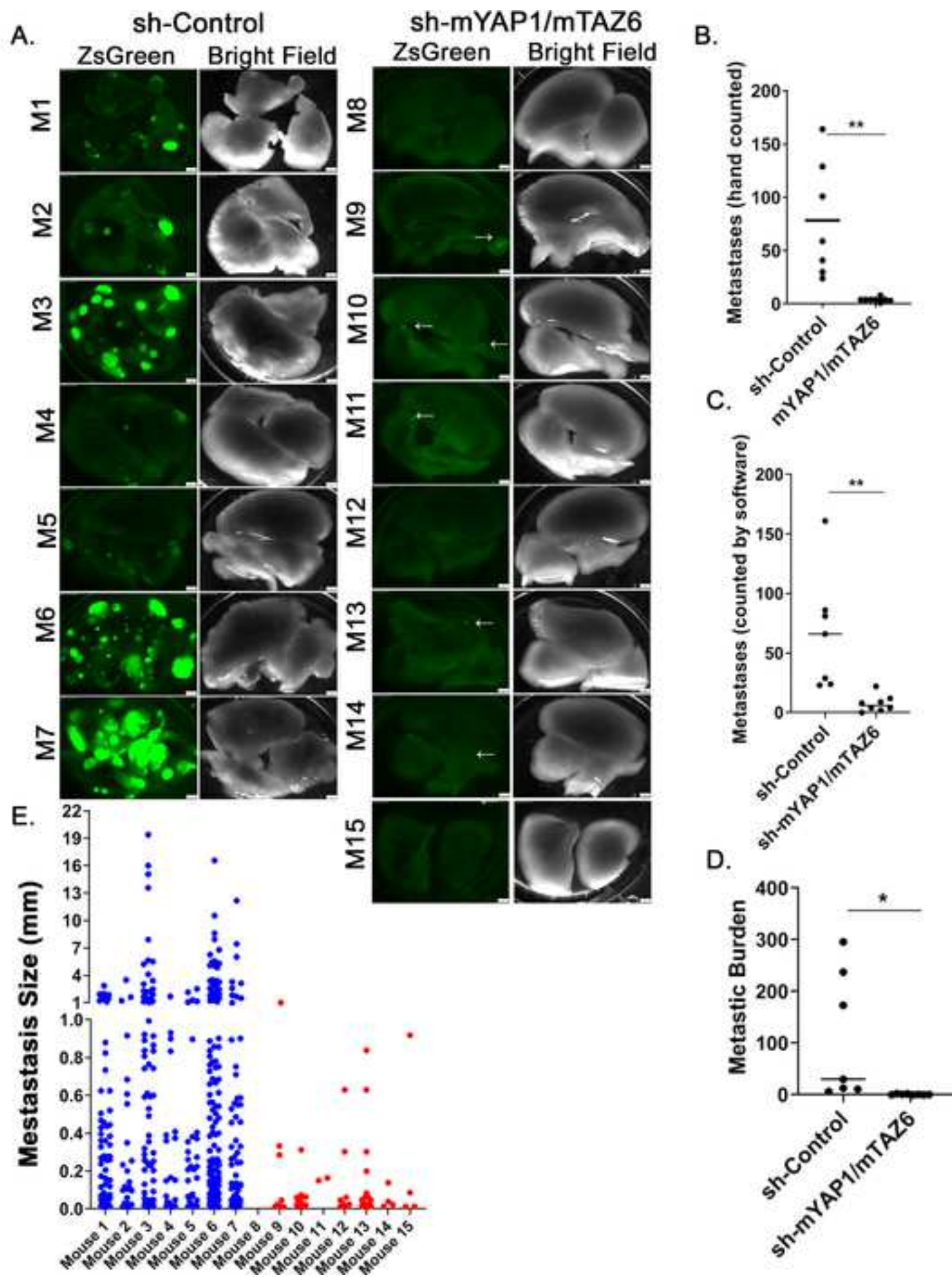932 576-590 (2011).
933

Figure 1

Figure 2

Click here to access/download;Figure;Figure 2.psd ⬇

Figure 3

A.
sh-Control
ZsGreen   Bright Field

sh-mRPA3
ZsGreen   Bright Field

M1
M2
M3
M4
M5
M6

M9
M10
M11
M12
M13
M14
M15
M16

B.

**

Metastases (hand counted)

sh-Control   sh-mRPA3-431

C.

**

Metastases (counted by software)

sh-Control   mRPA3-431

D.

#

Metastic Burden

sh-Control   mRPA3-431

E.

Mestastasis Size (mm)

Mouse 1 Mouse 2 Mouse 3 Mouse 4 Mouse 5 Mouse 6 Mouse 9 Mouse 10 Mouse 11 Mouse 12 Mouse 13 Mouse 14

Figure 4

Click here to access/download;Figure;Figure 4.psd ⬇

Figure 5

Table of Materials

Name of Material/ Equipment	Company	Catalog Number
10% SDS-PAGE Gel		
2.5% Trypsin	Gibco	15090-046
96 well flat bottom white assay plate	Corning	3922
Alcohol wipes		
BALB/C mice (female, 6 weeks)	Taconic	BALB-F
BSA regular	VWR Ameresco	97061-416
Cell lysis buffer	Cell Signaling	
Celltreat Syringe Filters, PES 30mm, 0.45 µm	Celltreat	40-229749-CS
CO_2 and euthanasia chamber		
Dual-luciferase reporter assay kit	Promega	E1960
Dulbecco's phosphate buffered saline	Himedia	TS1006
EDTA	VWR	97061-406
FBS 100% US origin	VWR	97068-085
Fujifilm LAS-3000 gel imager	Fujifilm	
GAPDH(14C10) Rabibit mAb	Cell Signaling	2118
Goat anti-rabbit IgG (H+L) Secondary Antibody, HRP conjugate	Thermo Scientific	31460
Human embryonic kidney cells, HEK-293FT	Invitrogen	R70007
HyClone DMEM/High clucose	GE Healthcare life sciences	SH30243.01
Hygromycin B, Ultra Pure Grade	VWR Ameresco	97064-810
I3-P/i3 Multi-Mode Microplate/EA	Molecular devices	
Imagej		
Immuno-Blot PVDF Membrane	Biorad	1620177
Isoflurane		
IVIS Lumina XRMS In Vivo Imaging System (*in vivo* live animal imaging device)	PerkinElmer	CLS136340
Leica M205 FA & Lecia DCF3000 G (GFP and bright field filters)	Leica Microsystems	
L-Glutamine	Gibco	25030-081
Lipofectamine 3000	Life technologies	L3000008
Living Image 3.2 (image software program)	PerkinElmer	
Mouse breast cancer cells, 4T1	Karmanos Cancer Institute	Aslakson, CJ et al.,1992

Multi-Gauge version 3.0	Fujifilm	
Opti-MEM (transfection buffer)	Gibco	31985-062
Penicillin Streptomycin	Gibco	15140-122
Pierce BCA protein assay kit	Thermo Scientific	23225
Pierce Phosphatase Inhibitor Mini Tablets	Thermo Scientific	A32957
Pierce Protease Inhibitor Mini Tablets	Thermo Scientific	A32953
Polybrene (hexadimethrine bromide)	Sigma-Aldrich	45-H9268
Puromycin	Sigma-Aldrich	45-P7255
Rodent restrainer		
SDS-PAGE running buffer		
TAZ (V3886) Antibody	Cell Signaling	4883
TBST buffer		
TC20 automated cell counter	Bio-Rad	
Vectors		
VWR Inverted Fluorescence Microscope	VWR	89404-464
Western transfer buffer		
XenoLight D-Luciferin K+ Salt	PerkinElmer	122799
X-tremeGENE 9 DNA transfection reagent (lipid solution for transfection)	Roche	6365787001
YAP (D8H1X) XP Rabbit mAb	Cell Signaling	14074

Comments/Description

For western blot

Trypsin for tissue culture

For measuring luciferase and renilla signal in cultured cells

For sterolizing the injection site before tail vein injecitons

For tail vein metastatic colonization and burden assays

For western blot

For collecting protien samples

For filtering viral supernatant

For euthanasing the mice

For measuring luciferase and renilla signal in cultured cells

For PBS

Used to dilute trypsin for tissue culture

Component of complete growth media

For western blot

For western blot

For western blot

Cell line used for packging virus

Component of complete growth media

For antibiotic selection of infected cells

For measuring luciferase and renilla signal in cultured cells

Used for image analysis of lung metastases: threshold set to 25 & 100

For western blot

For mouse anesthesia

For *in vivo* imaging of metastatic burden

Microscope and camera for visualing, counting and taking pcitures of metastases in the lungs; 10X magnifacation, 3.5 sec exposure, 1.4 gain

Component of complete growth media

For YAP/TAZ-TEAD reporter transfection

Software for IVIS

Mouse metastatic breast cance cell line

Software for quantifying western blot band intensity
For packaging virus and transfection
Component of complete growth media
For quantifying protein concentration
Added to cell lysis buffer
Added to cell lysis buffer
For infection
For antibiotic selection of infected cells
For restraining mice during tail vein injeciton
For western blot
For western blot
For western blot
For counting cells
See Table 1 for complete list of vectors
For visualizing fluorescence in ZSGreen labeled cells
For western blot
Substrate injected into mice for in vivo bioluminescent IVIS images
For packaging virus
For western blot

Editorial Comments:

• Please take this opportunity to thoroughly proofread the manuscript to ensure that there are no spelling or grammatical errors.
We have proofread the document to the best of our abilities to ensure that there are no spelling or grammatical errors.

• **Protocol Detail:** Please note that your protocol will be used to generate the script for the video, and must contain everything that you would like shown in the video.

1) 2.1: What is the composition of the complete media?
Media composition added in Step 2.1 **(Page 4).**

2) 2.3, 2.7.4, 3.2.2: Describe the trypsinization, e.g., how much trypsin and for how long? How is trypsin neutralized?
Trypsinization was described for **Steps 2.3, 2.7.4, and 4.2.2 (previously Step 3.2.2).**

3) 2.5: mention magnification, lens N.A., excitation and emission filters.
Added to **Steps 2.5** and **7.4**

4) 2.6: in order to film this all steps must be describe. Please expand this step. Do you image to confirm luciferase activity?
Steps 2.6.1-2.6.3 were added to describe this **(Page 4)**. We use a commercially available luciferase activity kit and measure the luciferase signal with a plate reader.

5) 3.2.3: what is the counting method?
An automated cell counter is used. We have added this in **Step 4.23** (**Page 7**)

• **References:** Please spell out journal names.
Done. Please note, we turned track changes off when updating the references.

• **Commercial Language:** JoVE is unable to publish manuscripts containing commercial sounding language, including trademark or registered trademark symbols (TM/R) and the mention of company brand names before an instrument or reagent. Examples of commercial sounding language in your manuscript are IVIS, IVIS Spectrum, Extremegene, Living Image.
All trademark and commercial language was replaced with generic names throughout.

• If your figures and tables are original and not published previously or you have already

obtained figure permissions, please ignore this comment. If you are re-using figures from a previous publication, you must obtain explicit permission to re-use the figure from the previous publisher (this can be in the form of a letter from an editor or a link to the editorial policies that allows you to re-publish the figure). Please upload the text of the re-print permission (may be copied and pasted from an email/website) as a Word document to the Editorial Manager site in the "Supplemental files (as requested by JoVE)" section. Please also cite the figure appropriately in the figure legend, i.e. "This figure has been modified from [citation]."

NA

Comments from Peer-Reviewers:

Reviewer #1:
Manuscript Summary:
Authors describe a useful protocol which enables researchers to investigate the effect of genetic modulation of key metastasis regulators using in vivo bioluminescence and fluorescence imaging.

Major Concerns:
1. Section 4.4.5
BLI quantification should be conducted when peak signal is reached. In some animals this may occur prior to 10 minutes. I suggest initiating imaging immediately and continuing to collect images until peak signal is achieved. Using the protocol as spelled out here the mouse would not be placed in the IVIS until 15 min post-ip injection.
We agree with the reviewer that this is the best way to collect images and have changed the protocol accordingly (**See Step 6.5**).

2. Overall comment
Authors should suggest that in vitro fluorescence and bioluminescence be compared between cells that have just received reporter genes vs those that also had an additional gene of interest manipulated. For simple data interpretation the fluorescence brightness or luciferase activity should be approximately equivalent across both populations. If genetic manipulation results in a sub-population that has altered reporter expression from the original cells than results may be interpreted inappropriately. In vitro proliferation assays should also be used to demonstrate that genetic manipulation has not altered innate cell proliferation rates in vitro before cells are applied in vivo.
We have added a step to the protocol **(Step 2.5-2.6)** to test luminescence and fluorescence of cells prior to injection and have discussed this potential issue in the modifications and trouble shooting section on **(Page 15)**. We suggest *in vitro* proliferation assays in the discussion on **(Page 16)**.

Minor Concerns:

1. Page 3 line 72

Grammatical correction: in a spontaneous metastasis models

Thank you. We have fixed this and they are now references 7-8.

2. Methods section 2

As the lentiviral transductions proposed include a fluorescent protein, authors may suggest performing fluorescence-activated cell sorting to select appropriately transduced cells in lieu of drug selection. This option eliminates the need to confer drug resistance and also provides the opportunity to select a subpopulation of cells with equivalent fluorescence intensity which in turn may make final fluorescent stereomicroscope data analysis easier to interpret.

A note was added to suggest this alternative after **Step 2.3**

3. Section 2.2

Why was hexadimethrine bromide chosen as a transduction agent as opposed to other choices? Eg polybrene.

JOVE policy prevents use of trademarked names, so we used hexadimethrine bromide in the protocol, but indicated it was polybrene in the Table Of Materials.

4. Section 4.1.3

Field of view C also provides view of the entire mouse body without zooming out nearly as much.

A note was added after **Step 5.7** and **Step 6.1.3.**

5. Section 4.4.1

Some d-luciferin manufacturers suggest resuspension in D-PBS formulation rather than PBS.

We used D-PBS, but did not indicate this. This was corrected.

6. Section 5

If another choice of euthanasia method is used (for example isoflurane overdose) then it opens up the opportunity for full blood clearance using buffer (saline, PBS or HBSS) perfusion. Full blood clearance would eliminate the potential for RBC autofluorescence.

We have discussed this in the discussion on **Page 18.**

7. Section 6.2

Explain why counts are the preferred units for fluorescent images. Also, for BLI data images should be compared at peak signal and authors should consider providing advice on what units to use (ie total flux or average radiance).

We consulted the manufacturer of the imaging device and they recommend images are first changed to "Radiance" for bioluminescent data and "Efficiency" for fluorescent data. We indicted in the protocol (**step 8.4**) and the discussion on **page 17**, that when quantifying metastatic burden in a given an ROI to use the "total flux" value for bioluminescence and "total efficiency %" value for fluorescence. We have also changed the units in **Figures 2B-D and 4D-F** to properly reflect the units used and plotted.

We changed the protocol **(now Step 8.2)** to indicate that BLI images should be compared at peak signal.

8. Modifications section

Authors should inform that while R.luciferase and F.luciferase can be used in the same animal models using their specific substrates, imaging both luciferases cannot be performed simultaneously as the IVIS cannot differentiate light originating from specific luciferase species. Thus, authors should warn that imaging for each luciferase be performed separately with adequate time delay such that signal from one luciferase is fully extinguished prior to imaging with the second.

This was added on **Page 18.**

Reviewer #2:

Manuscript Summary:

This manuscript provides a very granular, step-by-step protocol to perform in vivo imaging of luciferase/fluorescent protein-labelled tumor cells during an experimental metastasis assay. In particular, the authors provide a good example of a "positive result" where the knock-down of a gene (suspected of regulating metastasis) affects metastatic progression, as observed by in vivo luminescence/fluorescence imaging. It is also useful to know the type of variation from mouse to mouse can be observed in both control and test groups. It was pleasure reviewing the manuscript, and we look forward to seeing the article in press.

Major Concerns:

No major concerns.

Minor Concerns:

1. Line 75. Reference #6 refers to a very specific application of the experimental metastasis model to study lung tissue/tumor cells by microscopy ex vivo. Although Lizardo et al used the experimental metastasis model as part of their protocol paper, it would be better to include or add alongside the following references:

a) "Go-to" reference of in vivo models of metastasis by Danny Welch PMID: 9174129. Welch discusses the theory (pros and cons) behind various in vivo models of metastasis including experimental metastasis assays.

b) A more granular protocol paper for how to do an experimental metastasis assay would be by Mohanty and Xu (2010), also in JOVE. PMID: 20811329

Thank you for your suggestion. We have inserted these references.

2. Line 218. Write a sentence or two with respect to the optimal number of cells to be injected. For example: If too many cells are injected, the lungs will be overrun by metastatic tumor burden and the effects of the intervention may be masked. Too little of a number, and metastases may not form at all. Therefore a preliminary experiment which follows the metastatic progression from a variety of doses of cells injected should be performed. We have inserted an optimization step **(Step 3)** in the protocol that describes the optimization of cell number to obtain the desired metastatic burden and length of experiment. This was also added to the discussion on **Page 17.**

3. Line 252. Step 3.3.5. To warm up the tail, you can also add: "For immunodeficient strains of mice, within a sterile biological hood, pre-warm mice by adding a heating-pad under half of the cage, and place a heating-lamp over half the cage 20 minutes prior to injection." A note was inserted after **Step 4.3.4** suggesting this

4. Line 337. Step 5.1. It's probably more public friendly to say: "Euthanize mice according to standard institutional guidelines." We agree and have made the change (now **Step 7.1**).

Reviewer #3:
Manuscript Summary:
Submitted manuscript of JSA Warren et al. describes methods for dual labeling and in vivo tracing of mouse 4T1 cells to detect and monitor growth of lung metastases in syngeneic mouth models. This is important approach in tumor biology field which allows to identify and investigate multiple proteins involved in the regulation of metastases. Methods are described in details which seems sufficient for reproduction of results. However several issues should be resolved before further consideration:

Major Concerns:
1. The only type of metastases, described in the manuscript are lung metastases from the breast cancer cells. This should be reflected in the protocol and the title of manuscript, because other potential metastatic locations (liver, brain, bones etc) were either not assessed or are restricted by the given mode of tumor cell injection (tail IV) We altered the title and text to indicate that this was a protocol to assay metastasis to the lungs. We also indicated in the Discussion that the protocol can be altered for use with intracardiac and portal vein injections to assay metastasis to other organs.

2. Similarly, protocols should clearly state that these are mouse 4T1 cells, not the broad definition of "cancer cells". Many details here are cell-specific and their potential application to other cell types should be first demonstrated. Cancer cells was changed to 4T1 cells in several places as suggested.

3. Section 2 should be clarified from the point of view what vectors were used for the transduction of 4T1 cells and how many different vectors were used. My understanding is that there were just two vectors (MSCV-Zsgreen-2A-Puro-shmYAP1/mTAZ6 or MSCV-Zsgreen-2A-Puro-mRPA3 and pHAGE-Luc-IRES-Hygro). Why 3rd vector is mentioned for gene suppression? (row 160).

We have intentionally left Step 2 as a general approach for labeling cancer cells first and then altering the gene of interest as this is the best way to do the experiment. However, since our existing miR30 vectors also delivered ZsGreen we used the alternative approach in the representative results. To clarify how the representative experiments were done, we added schematic in **Figures 2 and 4**. We also indicated in the representative results that we used a modified approach compared to the protocol **(Page 11)**.

4. Figure with maps of vectors will be very helpful
Schematics with vectors maps were added to **Figures 2 and 4**

5. It is not clear, whether cells are transduced by both Luc and Zsgreen-shRNA vectors simultaneously or sequentially? And whether they are selected in the media with either both antibiotics (Puro+Hygro) or first in one and then in the other? This should be described clearly with indication of concentrations and explanations why these concentrations were used.

As mentioned above, we wrote step 2 to be a general approach for stably labeling the cells since a protocol specific to our viral vectors for luciferase and ZsGreen would not be as helpful. However, we have added schematics to **Figures 2 and 4** describing how transduction and selection was done for the representative experiments. Antibiotics concentrations were added to figure legends for **Figures 2 and 4**.

6. Quantification of Luc activity (rows 186-187) should be explained in more details and equipment should be indicated.
The suggested steps were added **(steps 2.6.1-2.6.3)**.

7. How amount of 4T1 cells for tail vein injection (row 235) was justified? Did authors used other amounts?
We added an optimization step to the protocol **(Step 3)** to help determine the optimal cell number to inject into each mouse. For our representative results using 4T1 cells we previously determined the optimal cell number experimentally.

8. What authors mean by "the slope" of the growth curves (6.7-6.8)? Is that the part of the growth curve which corresponds to the logarithmic growth, or just the difference between first and last day of measurements? Should be explained clearly. Why Log10, not Log2 for growth curves?

We have now clarified in **Step 8.7.2** and on **Supplemental Table 2** and its legend that the slope is generated by fitting a line to all the transformed data points for each mouse. We also added the units for the slope to the plot of the slope values.

We used log10 rather than log2 because we felt it would be easier for people to interoperate, since 1 = 10, 10 = 100, etc. with a log10 transformation. A log2 transformation would generate larger numbers than a log10 transformation since you must multiply the log10 values by 0.30103 to change to log2 from log10. Thus, the values plotted on the log-transformed plots would be larger, the slopes would be larger, and the error would also be larger. However, the p values end up being the same, so statistically there is no difference between using a log10 or log2 transformation.

9. Again, what part of the curves was used for linear regression and how this part was selected? This seems very subjective

We have clarified the analysis in **Step 8.7** and **Supplamental Table 2** to indicate all datapoints for each mouse were used to generate the slope for each mouse. See above comment.

10. I am not sure that authors really quantified growth of individual metastatic colonies (Abstract and row 424), which should be done by the measurements of individual colonies sizes. In the presented experiments growth seems to go together with metastatic frequencies, but in the other models they may be regulated separately (Oshima G. et al., Sci Rep. 2015;5:10946)

We now indicate on **Page 2** of the Introduction and **Page 18** of the Discussion that IVIS cannot determine whether changes in metastatic burden are caused by changes in the size or number (or both) of metastases. This is why we counted by number and size as well. We added measurements of individual metastases to **Figures 3** and **5**. These data clearly show that the size of the metastases is smaller in the knockdown cells.

11. Why amount of mets in the control shRNA groups in two different experiments are almost log of magnitude different? (Figures 3B and 5B?)

We are not certain why this was the case, but suspect it is due to the inherent heterogeneity of the parental 4T1 cells. The control cells used in each experiment were generated independently at different times using different batches of control virus. We suspect that the infection/selection of the cells could enrich different populations from the heterogeneous parental line resulting in cells with different metastatic potential. We control for this variability in several ways. We always generate control and knockdown cells from the same population of cells (in this case 4T1-Luciferase) and using retroviruses packaged at the same time from the same population of HEK-293FT cells. This way the control and knockdown cells are as similar as possible. Both control and knockdown populations are prepared for injection and injected at the same time to reduce variability introduced by the handling/counting of the cells. We typically repeat all experiments 2x with 6-8 mice each to ensure that any observed differences resulting from knockdown are reproducible.

Collectively this helps us ensure that even if the total number of metastases differs between 2 experiments, the magnitude of reduction caused by the knockdown is consistent.

Minor Concerns:
check reference style
Corrected.

Other change: We removed a previous figure (Figure 2) which demonstrated the use of fluorescence to monitor metastatic burden in the same mice that bioluminescence was measured. We removed this figure because in an attempt to address reviewer comments about the units used to measure fluorescence, we contacted the manufacturer of the IVIS machine. During our discussion she told us that bioluminescence can sometimes be detected when measuring fluorescence, so we should never measure fluorescence in mice with detectable bioluminescence signal. For this reason, we could not be certain that all of the signal in the data was fluorescence, so we removed these data. However, we left the steps in the protocol that describe how to use fluorescence to monitor metastatic burden. We also indicated in the protocol that fluorescence should not be measured in mice with active bioluminescence signal.

Existing/Purchased/Gift vectors

Vector	Source
pCL-Eco	Addgene (#12371) [1]
VSVG	Hynes Lab [2]
psPAX2	Addgene (#12260)
gag/pol	Addgene (#14887)
pGL3-5xMCAT(SV)-49	Iain Farrance [3]
PRL-TK	Promega

New Vectors

Vector	Source Backbone	Source Insert	Target Gene
MSCV-Zsgreen-2A-Puro-sh-mCherry	MSCV-Zsgreen-2A-Puro-miR30 [2]	synthesized 97-mer	mCherry
MSCV-Zsgreen-2A-Puro-sh-mYAP1/mTAZ6	MSCV-Zsgreen-2A-Puro-miR30 [2]	synthesized 97-mer	mouse YAP
		synthesized 97-mer	mouse TAZ
MSCV-Zsgreen-2A-Puro-sh-mRPA3-431	MSCV-Zsgreen-2A-Puro-miR30 [2]	MSCV-Puro-2A-GFP-sh-mRPA3-431 BC [5]	mouse RPA3
pHAGE-Luciferase-IRES-Hygro	Generated using standard molecular bio		

97-mer Sequence
TGCTGTTGACAGTGAGCGACGAGTTCATCTACAAAGTTAATAGTGAAGCCACAGATGTATTAACTTTGTAGATGAACTCGCTGCCTACTGCCTCGGA
TGCTGTTGACAGTGAGCGAATGGAGAAGTTTACTACATAATAGTGAAGCCACAGATGTATTATGTAGTAAACTTCTCCATCTGCCTACTGCCTCGGA
TGCTGTTGACAGTGAGCGCCCAGAAGACTTCCTCAGCAACTAGTGAAGCCACAGATGTAGTTGCTGAGGAAGTCTTCTGGATGCCTACTGCCTCGGA

logy techniques.

	sh-Control					
Day	Mouse 1	Mouse 2	Mouse 3	Mouse 4	Mouse 5	Mouse 6
0	1.52E+06	1.25E+06	2.49E+06	5.39E+05	9.26E+05	5.61E+05
3	7.10E+04	8.34E+04	7.36E+04	1.49E+05	1.01E+05	8.67E+04
7	9.64E+04	5.62E+04	1.83E+05	3.51E+05	8.31E+04	2.79E+05
10	7.74E+05	3.01E+05	2.27E+06	6.93E+05	9.41E+04	3.16E+05
14	2.93E+06	7.09E+05	6.43E+07	3.75E+07	1.44E+05	2.14E+05
17	5.74E+06	9.90E+06	8.46E+07	1.87E+08	1.47E+05	3.55E+05
21	9.73E+06	2.35E+07	1.44E+08	2.25E+08	2.26E+05	1.87E+05

Log_{10} tr

	sh-Control					
Day (y1)	Mouse 1 (x1)	Mouse 2 (x2)	Mouse 3 (x3)	Mouse 4 (x4)	Mouse 5 (x5)	Mouse 6 (x6)
3	4.851074805	4.921218121	4.8670548	5.173477643	5.003029471	4.938219418
7	4.984257202	4.749890841	5.261976191	5.545183368	4.91981002	5.446226402
10	5.888797067	5.478710756	6.356408327	5.840983837	4.973543469	5.499687083
14	6.467163966	5.850339855	7.80827851	7.57391544	5.157456768	5.329601248
17	6.759063188	6.995635195	7.927216331	8.270678836	5.167612673	5.549983611
21	6.987934265	7.371437317	8.157758886	8.351216345	5.354300562	5.272769587

Slope of log_{10} transf

	sh-Control					
	Mouse 1	Mouse 2	Mouse 3	Mouse 4	Mouse 5	Mouse 6
Equation:	slope(ys,x1s)	slope(ys,x2s)	slope(ys,x3s)	slope(ys,x4s)	slope(ys,x5s)	slope(ys,x6s)
Slope:	0.133011358	0.154654331	0.208392172	0.207695404	0.021673999	0.014498027

Raw Data

	sh-mRPA3-431				
Mouse 9	Mouse 10	Mouse 11	Mouse 12	Mouse 13	Mouse 14
5.70E+05	1.19E+06	8.59E+05	5.69E+05	3.82E+05	1.05E+06
9.50E+04	9.28E+04	9.73E+04	6.97E+04	6.21E+04	7.02E+04
1.08E+05	4.88E+04	9.34E+04	1.56E+05	5.44E+04	1.46E+05
7.06E+04	6.37E+04	7.42E+04	6.23E+04	7.10E+04	6.26E+04
1.05E+05	1.23E+05	1.12E+05	1.37E+05	1.03E+05	1.28E+05
1.20E+05	6.85E+04	1.01E+05	1.29E+05	1.84E+06	1.26E+05
1.36E+05	1.34E+05	7.69E+04	1.30E+05	1.25E+06	1.29E+05

ansformed data (formula: =LOG10(cell))

	sh-mRPA3-431				
Mouse 9 (x7)	Mouse 10 (x8)	Mouse 11 (x9)	Mouse 12 (x10)	Mouse 13 (x11)	Mouse 14 (x12)
4.977632165	4.967735132	4.988157473	4.843295083	4.79302166	4.846584503
5.034227261	4.688686724	4.970114322	5.193124598	4.7355989	5.163459552
4.848804701	4.804412059	4.870403905	4.794139356	4.8509524	4.796643704
5.022840611	5.089551883	5.049992857	5.137037455	5.014100322	5.105850674
5.07809415	4.835627166	5.005609445	5.111598525	6.264345507	5.101747074
5.133219457	5.128076013	4.88592634	5.114944416	6.096214585	5.110252917

ormed data (formula: =SLOPE(known_ys,known_xs))

	sh-mRPA3-431				
Mouse 9	Mouse 10	Mouse 11	Mouse 12	Mouse 13	Mouse 14
slope(ys,x7s)	slope(ys,x8s)	slope(ys,x9s)	slope(ys,x10s)	slope(ys,x11s)	slope(ys,x12s)
0.008944054	0.012491135	-0.001742849	0.012377317	0.089539842	0.012194851

Mouse 15	Mouse 16
5.57E+05	1.17E+05
1.18E+05	7.91E+04
1.60E+05	1.22E+05
7.29E+04	8.64E+04
1.00E+05	1.94E+05
1.21E+05	4.40E+05
1.01E+05	2.20E+06

Mouse 15 (x13)	Mouse 16 (x14)
5.071513805	4.898176483
5.202760687	5.084933575
4.862727528	4.936564005
5.000434077	5.287577809
5.083824996	5.643452676
5.004321374	6.341830057

Mouse 15	Mouse 16
slope(ys,x13s)	slope(ys,x14s)
-0.004199987	0.074943206

jove
JOURNAL OF VISUALIZED EXPERIMENTS

1 Alewife Center #200
Cambridge, MA 02140
tel. 617.945.9051
www.jove.com

ARTICLE AND VIDEO LICENSE AGREEMENT

Title of Article:	Combined use of tail vein metastasis assays and real-time IVIS imaging to quantify metastatic colonization and burden
Author(s):	Janine S. A. Warren, Paul J. Feustel, John M. Lamar

Item 1: The Author elects to have the Materials be made available (as described at http://www.jove.com/publish) via:

☑ Standard Access   ☐ Open Access

Item 2: Please select one of the following items:

☑ The Author is **NOT** a United States government employee.

☐ The Author is a United States government employee and the Materials were prepared in the course of his or her duties as a United States government employee.

☐ The Author is a United States government employee but the Materials were NOT prepared in the course of his or her duties as a United States government employee.

ARTICLE AND VIDEO LICENSE AGREEMENT

1.   **Defined Terms.** As used in this Article and Video License Agreement, the following terms shall have the following meanings: "**Agreement**" means this Article and Video License Agreement; "**Article**" means the article specified on the last page of this Agreement, including any associated materials such as texts, figures, tables, artwork, abstracts, or summaries contained therein; "**Author**" means the author who is a signatory to this Agreement; "**Collective Work**" means a work, such as a periodical issue, anthology or encyclopedia, in which the Materials in their entirety in unmodified form, along with a number of other contributions, constituting separate and independent works in themselves, are assembled into a collective whole; "**CRC License**" means the Creative Commons Attribution-Non Commercial-No Derivs 3.0 Unported Agreement, the terms and conditions of which can be found at: http://creativecommons.org/licenses/by-nc-nd/3.0/legalcode; "**Derivative Work**" means a work based upon the Materials or upon the Materials and other pre-existing works, such as a translation, musical arrangement, dramatization, fictionalization, motion picture version, sound recording, art reproduction, abridgment, condensation, or any other form in which the Materials may be recast, transformed, or adapted; "**Institution**" means the institution, listed on the last page of this Agreement, by which the Author was employed at the time of the creation of the Materials; "**JoVE**" means MyJove Corporation, a Massachusetts corporation and the publisher of The Journal of Visualized Experiments; "**Materials**" means the Article and / or the Video; "**Parties**" means the Author and JoVE; "**Video**" means any video(s) made by the Author, alone or in conjunction with any other parties, or by JoVE or its affiliates or agents, individually or in collaboration with the Author or any other parties, incorporating all or any portion

of the Article, and in which the Author may or may not appear.

2.   **Background.** The Author, who is the author of the Article, in order to ensure the dissemination and protection of the Article, desires to have the JoVE publish the Article and create and transmit videos based on the Article. In furtherance of such goals, the Parties desire to memorialize in this Agreement the respective rights of each Party in and to the Article and the Video.

3.   **Grant of Rights in Article.** In consideration of JoVE agreeing to publish the Article, the Author hereby grants to JoVE, subject to **Sections 4** and **7** below, the exclusive, royalty-free, perpetual (for the full term of copyright in the Article, including any extensions thereto) license (a) to publish, reproduce, distribute, display and store the Article in all forms, formats and media whether now known or hereafter developed (including without limitation in print, digital and electronic form) throughout the world, (b) to translate the Article into other languages, create adaptations, summaries or extracts of the Article or other Derivative Works (including, without limitation, the Video) or Collective Works based on all or any portion of the Article and exercise all of the rights set forth in (a) above in such translations, adaptations, summaries, extracts, Derivative Works or Collective Works and (c) to license others to do any or all of the above. The foregoing rights may be exercised in all media and formats, whether now known or hereafter devised, and include the right to make such modifications as are technically necessary to exercise the rights in other media and formats. If the "Open Access" box has been checked in **Item 1** above, JoVE and the Author hereby grant to the public all such rights in the Article as provided in, but subject to all limitations and requirements set forth in, the CRC License.

612542.6   For questions, please contact us at submissions@jove.com or +1.617.945.9051.

1 Alewife Center #200
Cambridge, MA 02140
tel. 617.945.9051
www.jove.com

4.   **Retention of Rights in Article.** Notwithstanding the exclusive license granted to JoVE in **Section 3** above, the Author shall, with respect to the Article, retain the non-exclusive right to use all or part of the Article for the non-commercial purpose of giving lectures, presentations or teaching classes, and to post a copy of the Article on the Institution's website or the Author's personal website, in each case provided that a link to the Article on the JoVE website is provided and notice of JoVE's copyright in the Article is included. All non-copyright intellectual property rights in and to the Article, such as patent rights, shall remain with the Author.

5.   **Grant of Rights in Video – Standard Access.** This **Section 5** applies if the "Standard Access" box has been checked in **Item 1** above or if no box has been checked in **Item 1** above. In consideration of JoVE agreeing to produce, display or otherwise assist with the Video, the Author hereby acknowledges and agrees that, Subject to **Section 7** below, JoVE is and shall be the sole and exclusive owner of all rights of any nature, including, without limitation, all copyrights, in and to the Video. To the extent that, by law, the Author is deemed, now or at any time in the future, to have any rights of any nature in or to the Video, the Author hereby disclaims all such rights and transfers all such rights to JoVE.

6.   **Grant of Rights in Video – Open Access.** This **Section 6** applies only if the "Open Access" box has been checked in **Item 1** above. In consideration of JoVE agreeing to produce, display or otherwise assist with the Video, the Author hereby grants to JoVE, subject to **Section 7** below, the exclusive, royalty-free, perpetual (for the full term of copyright in the Article, including any extensions thereto) license (a) to publish, reproduce, distribute, display and store the Video in all forms, formats and media whether now known or hereafter developed (including without limitation in print, digital and electronic form) throughout the world, (b) to translate the Video into other languages, create adaptations, summaries or extracts of the Video or other Derivative Works or Collective Works based on all or any portion of the Video and exercise all of the rights set forth in (a) above in such translations, adaptations, summaries, extracts, Derivative Works or Collective Works and (c) to license others to do any or all of the above. The foregoing rights may be exercised in all media and formats, whether now known or hereafter devised, and include the right to make such modifications as are technically necessary to exercise the rights in other media and formats. For any Video to which this **Section 6** is applicable, JoVE and the Author hereby grant to the public all such rights in the Video as provided in, but subject to all limitations and requirements set forth in, the CRC License.

7.   **Government Employees.** If the Author is a United States government employee and the Article was prepared in the course of his or her duties as a United States government employee, as indicated in **Item 2** above, and any of the licenses or grants granted by the Author hereunder exceed the scope of the 17 U.S.C. 403, then the rights granted hereunder shall be limited to the maximum rights permitted under such statute. In such case, all provisions contained herein that are not in conflict with such statute shall remain in full force and effect, and all provisions contained herein that do so conflict shall be deemed to be amended so as to provide to JoVE the maximum rights permissible within such statute.

8.   **Protection of the Work.** The Author(s) authorize JoVE to take steps in the Author(s) name and on their behalf if JoVE believes some third party could be infringing or might infringe the copyright of either the Author's Article and/or Video.

9.   **Likeness, Privacy, Personality.** The Author hereby grants JoVE the right to use the Author's name, voice, likeness, picture, photograph, image, biography and performance in any way, commercial or otherwise, in connection with the Materials and the sale, promotion and distribution thereof. The Author hereby waives any and all rights he or she may have, relating to his or her appearance in the Video or otherwise relating to the Materials, under all applicable privacy, likeness, personality or similar laws.

10.   **Author Warranties.** The Author represents and warrants that the Article is original, that it has not been published, that the copyright interest is owned by the Author (or, if more than one author is listed at the beginning of this Agreement, by such authors collectively) and has not been assigned, licensed, or otherwise transferred to any other party. The Author represents and warrants that the author(s) listed at the top of this Agreement are the only authors of the Materials. If more than one author is listed at the top of this Agreement and if any such author has not entered into a separate Article and Video License Agreement with JoVE relating to the Materials, the Author represents and warrants that the Author has been authorized by each of the other such authors to execute this Agreement on his or her behalf and to bind him or her with respect to the terms of this Agreement as if each of them had been a party hereto as an Author. The Author warrants that the use, reproduction, distribution, public or private performance or display, and/or modification of all or any portion of the Materials does not and will not violate, infringe and/or misappropriate the patent, trademark, intellectual property or other rights of any third party. The Author represents and warrants that it has and will continue to comply with all government, institutional and other regulations, including, without limitation all institutional, laboratory, hospital, ethical, human and animal treatment, privacy, and all other rules, regulations, laws, procedures or guidelines, applicable to the Materials, and that all research involving human and animal subjects has been approved by the Author's relevant institutional review board.

11.   **JoVE Discretion.** If the Author requests the assistance of JoVE in producing the Video in the Author's facility, the Author shall ensure that the presence of JoVE employees, agents or independent contractors is in accordance with the relevant regulations of the Author's institution. If more than one author is listed at the beginning of this Agreement, JoVE may, in its sole

612542.6   For questions, please contact us at submissions@jove.com or +1.617.945.9051.

discretion, elect not take any action with respect to the Article until such time as it has received complete, executed Article and Video License Agreements from each such author. JoVE reserves the right, in its absolute and sole discretion and without giving any reason therefore, to accept or decline any work submitted to JoVE. JoVE and its employees, agents and independent contractors shall have full, unfettered access to the facilities of the Author or of the Author's institution as necessary to make the Video, whether actually published or not. JoVE has sole discretion as to the method of making and publishing the Materials, including, without limitation, to all decisions regarding editing, lighting, filming, timing of publication, if any, length, quality, content and the like.

12.   **Indemnification.** The Author agrees to indemnify JoVE and/or its successors and assigns from and against any and all claims, costs, and expenses, including attorney's fees, arising out of any breach of any warranty or other representations contained herein. The Author further agrees to indemnify and hold harmless JoVE from and against any and all claims, costs, and expenses, including attorney's fees, resulting from the breach by the Author of any representation or warranty contained herein or from allegations or instances of violation of intellectual property rights, damage to the Author's or the Author's institution's facilities, fraud, libel, defamation, research, equipment, experiments, property damage, personal injury, violations of institutional, laboratory, hospital, ethical, human and animal treatment, privacy or other rules, regulations, laws, procedures or guidelines, liabilities and other losses or damages related in any way to the submission of work to JoVE, making of videos by JoVE, or publication in JoVE or elsewhere by JoVE. The Author shall be responsible for, and shall hold JoVE harmless from, damages caused by lack of sterilization, lack of cleanliness or by contamination due to

the making of a video by JoVE its employees, agents or independent contractors. All sterilization, cleanliness or decontamination procedures shall be solely the responsibility of the Author and shall be undertaken at the Author's expense. All indemnifications provided herein shall include JoVE's attorney's fees and costs related to said losses or damages. Such indemnification and holding harmless shall include such losses or damages incurred by, or in connection with, acts or omissions of JoVE, its employees, agents or independent contractors.

13.   **Fees.** To cover the cost incurred for publication, JoVE must receive payment before production and publication of the Materials. Payment is due in 21 days of invoice. Should the Materials not be published due to an editorial or production decision, these funds will be returned to the Author. Withdrawal by the Author of any submitted Materials after final peer review approval will result in a US$1,200 fee to cover pre-production expenses incurred by JoVE. If payment is not received by the completion of filming, production and publication of the Materials will be suspended until payment is received.

14.   **Transfer, Governing Law.** This Agreement may be assigned by JoVE and shall inure to the benefits of any of JoVE's successors and assignees. This Agreement shall be governed and construed by the internal laws of the Commonwealth of Massachusetts without giving effect to any conflict of law provision thereunder. This Agreement may be executed in counterparts, each of which shall be deemed an original, but all of which together shall be deemed to me one and the same agreement. A signed copy of this Agreement delivered by facsimile, e-mail or other means of electronic transmission shall be deemed to have the same legal effect as delivery of an original signed copy of this Agreement.

A signed copy of this document must be sent with all new submissions. Only one Agreement is required per submission.

CORRESPONDING AUTHOR

Name:	John M. Lamar
Department:	Department of Molecular and Cellular Physiology
Institution:	Albany Medical College
Title:	Associate Professor

Signature:	*John Lamar*	Date:	08/16/2019

Please submit a **signed** and **dated** copy of this license by one of the following three methods:
1. Upload an electronic version on the JoVE submission site
2. Fax the document to +1.866.381.2236
3. Mail the document to JoVE / Attn: JoVE Editorial / 1 Alewife Center #200 / Cambridge, MA 02140

612542.6   For questions, please contact us at submissions@jove.com or +1.617.945.9051.

Signature Certificate

Document Ref.: 5ILKF-SK2WJ-G42CI-FT2XZ

Document signed by:

John Lamar

Verified E-mail:
lamarj@amc.edu

IP: 66.109.35.61   Date: 16 Aug 2019 18:19:33 UTC

John Lamar

Document completed by all parties on:
16 Aug 2019 18:19:33 UTC

Page 1 of 1

Signed with **PandaDoc.com**

PandaDoc is the document platform that boosts your company's revenue by accelerating the way it transacts.